UNIVERSIDAD NACIONAL AUTÓNOMA DE MÉXICO

PROGRAMA DE MAESTRÍA Y DOCTORADO EN INGENIERÍA
MECÁNICA – TERMOFLUIDOS

RHEOLOGICAL CHARACTERIZATION OF DYSPHAGIA DIET FOODS

TESIS

QUE PARA OPTAR POR EL GRADO DE:

MAESTRA EN INGENIERÍA

PRESENTA:

I.A. MÓNICA YOSELÍN GARCÍA CORTÉS

TUTOR

DRA. MARÍA SOLEDAD CÓRDOVA AGUILAR

CENTRO DE CIENCIAS APLICADAS Y DESARROLLO TECNOLÓGICO, UNAM

COTUTOR

DR. GABRIEL ASCANIO GASCA

CENTRO DE CIENCIAS APLICADAS Y DESARROLLO TECNOLÓGICO, UNAM

MÉXICO, D. F. ENERO 2014

JURADO ASIGNADO:

Presidente:	DR. FEDERICO MENDEZ LAVIELLE
Secretario:	DR. FRANCISCO JAVIER SOLORIO ORDAZ
Vocal:	DRA. MARÍA SOLEDAD CÓRDOVA AGUILAR
1er. Suplente:	DR. GABRIEL ASCANIO GASCA
2do. Suplente:	DR. ÁNGEL ENRIQUE CHÁVEZ CASTELLANO

Lugares donde se realizó la tesis:

CENTRO DE CIENCIAS APLICADAS Y DESARROLLO TECNOLÓGICO, UNIVERSIDAD NACIONAL AUTÓNOMA DE MÉXICO, CIUDAD UNIVERSITARIA, D. F., MÉXICO.

DEPARTAMENTO DE INGENIERÍA QUÍMICA, QUÍMICA FÍSICA Y QUÍMICA ORGÁNICA, UNIVERSIDAD DE HUELVA, CAMPUS EL CARMEN, HUELVA, ESPAÑA.

TUTOR DE TESIS:	**COTUTOR DE TESIS:**
Dra. María Soledad Córdova Aguilar	Dr. Gabriel Ascanio Gasca
---	---
FIRMA	**FIRMA**

Para mi familia por el gran apoyo que siempre me brindan.

Este trabajo se desarrolló bajo la asesoría de la Dra. María Soledad Córdova Aguilar, en el laboratorio de Ingeniería de Proceso del Departamento de Instrumentación y Medición del Centro de Ciencias Aplicadas y Desarrollo Tecnológico de la UNAM.

Se agradece al CONACyT por la beca otorgada durante el desarrollo del proyecto. De igual forma, se agradece a la UNAM y a la empresa Fresenius-Kabi Deutschland GmbH por el apoyo recibido y por la estancia en el laboratorio de Reología en la Universidad de Huelva, España.

Se agradece al Dr. Gabriel Ascanio Gasca por la asesoría y el apoyo técnico otorgado.

Se agrade la asistencia técnica de: Mtro. Jonathan Arenas Aguirre, Dra. Mirta Viviana Jozami, Dr. Oliver Cortes Pérez y Dr. Enrique Soto Castruita.

Resumen

La Disfagia es un padecimiento que afecta la habilidad de un individuo para deglutir alimentos sólidos o líquidos. Se ha encontrado que proporcionar alimentos espesos a este tipo de pacientes puede disminuir el riesgo de desarrollar asfixia u otros problemas de salud. Como parte del diagnóstico se realiza un examen de videofluoroscopía con fluidos de contraste de diferentes viscosidades para conocer el nivel de espesamiento que es seguro para cada paciente.

En este trabajo se evaluó la viscosidad extensional, así como la viscosidad de corte y las propiedades viscoelásticas de un fluido de contraste tipo “spoon-thick”, de soluciones de leche espesadas con viscosificantes de uso alimentario y de dos alimentos comerciales para caracterizar y definir la conveniencia de recomendarlos en la dieta de pacientes con disfagia.

Se utilizó como viscosificantes goma xantana y pectina cítrica a diferentes concentraciones para espesar soluciones de leche. Las muestras que mostraron una viscosidad de corte similar a la del fluido de contraste fueron seleccionadas para medirles, junto con el fluido de contraste y los alimentos comerciales, la viscosidad extensional, el módulo elástico, el módulo viscoso, y el módulo de relajación de esfuerzo.

De acuerdo al estudio las soluciones de leche con goma xantana al 3.6% y 4.4% son las más adecuadas para pacientes que reaccionan bien al fluido de contraste tipo “spoon-thick”. Esto debido a que después de evaluar la viscosidad extensional de las muestras se observó que las viscosidades de las dos soluciones de leche con goma xantana fueron las más parecidas a la

viscosidad del fluido de contraste. Todas las muestras mostraron un comportamiento adelgazante tanto en flujo extensional como en corte. Los alimentos envasados y el fluido de contraste mostraron un comportamiento tipo gel, mientras que las soluciones de leche mostraron un comportamiento tipo solución polimérica.

Abstract

Dysphagia is a disorder that affects the patient's ability for swallowing solid or liquid foods. It has been found that thickening foods for these patients can diminishes the risk of developing any health problem. A videofluoroscopic evaluation is performed using contrast fluid with different viscosities with the purpose of establishing the safe thickening level for each patient.

This work aimed to evaluate the extensional viscosity as well as shear viscosity and viscoelastic properties of two pre-packed thickened foods, thickened milk solutions and a videofluoroscopic contrast fluid (spoon-thick consistency) in order to know the suitability of these foods for dysphagic patients.

Xanthan gum and citrus pectin were used at different concentrations to thick milk solutions. The samples that matched their shear viscosity with that of the contrast fluid were selected in order to measure, along with the contrast fluid and the pre-packed thickened foods, the extensional viscosity, elastic modulus, viscous modulus and stress relaxation modulus.

According to the study the milk solutions thickened with xanthan gum at 3.6% and 4.4% are the most suitable for patients who respond well to the contrast fluid with spoon-thick consistency. Although all the samples showed an extensional viscosity similar to that of the contrast fluid, the viscosity of the milk solutions with xanthan gum was the closest to the viscosity of the contrast fluid. All the samples showed a thinning behavior in extensional and shear flow. The pre-packed thickened foods and contrast fluid showed a weak gel-like behavior, while the thickened milk solutions showed a true polymer solution behavior.

Table of contents

List of tables

List of figures

List of abbreviations and symbols

ADA	American Dietetic Association
BBS	Barium sulphate suspension
δ	Loss angle
$\dot{\epsilon}$	Extension rate
γ	Strain
γ_0	Strain amplitude
$\bar{\gamma}$	Effective strain rate
$\dot{\gamma}$	Shear rate
G	Stress relaxation modulus
G'	Elastic modulus
G''	Viscous modulus
G^*	Complex modulus
h	Damping function
l	Fitting parameter
μ	Newtonian shear viscosity
μ_e	Newtonian extensional viscosity

η	Shear viscosity
η_e	Extensional viscosity
K_2	Fitting parameter
n	Flow behavior index
$\bar{\bar{\sigma}}$	Stress tensor
σ_0	Stress amplitude
t	Fitting parameter
Tr	Trouton ratio
ω	Angular frequency

1 Introduction

Dysphagia is a disorder that affects the ability for swallowing solid or liquid foods. It causes health problems like malnutrition, dehydration, aspiration, pneumonia and even death (Groher, 1997; Whelan, 2001).

It has been found that thickening foods diminishes the risk of developing any of these complications. Thus, there is a concern about the type of food and thickening level suitable for each patient.

Physicians perform a videofluoroscopic test for evaluation of swallowing, in which the patient swallows small portions of a contrast fluid and the transit bolus is observed by X-rays in real time. This evaluation is repeated with different thickened levels of the contrast fluid. Therefore, the physicians can recommend a diet with the same characteristics of the contrast fluid that solve well the swallowing patient problem.

An approach commonly used for making food for dysphagic patients is matching the shear viscosity of the food with that of the contrast fluid, in which the patient has no more swallowing disadvantages. However the bolus is not only subjected to shear deformations but also it is clear that the extensional strains also play an important role in the swallowing process as well as significantly in the sensory perception (Stading, Edrud, & Ekman, 2007).

Besides, it has been found a strong correlation between extensional viscosity and the perceived ease of swallowing (Wendin et al., 2010).

Nowadays, there is pre-packed thickened food ready-to-serve having a specific shear viscosity and according to the manufacturers they fulfill the nutritional requirements of the patient but no information is provided about the extensional viscosity. On the other hand, it is possible to use food thickeners to modify the shear viscosity of a wide variety of foodstuff to the level required by the patient although it is worth to mention that only it is measured the shear viscosity but not the extensional viscosity.

This work aims to evaluate the extensional viscosity of two pre-packed thickened foods, several thickened milk solutions and a contrast fluid in order to get insight about the suitability of these foods for dysphagic patients.

The two pre-packed thickened food were designed following the approach of matching the shear viscosity of the contrast fluid with spoon-thick consistency. Moreover, two food thickeners, xanthan gum and citrus pectin, were used at different concentrations to thick milk solutions in order to find the samples that match their shear viscosity with the one of the contrast fluid. All the products were also evaluated in terms of extensional viscosity and viscoelastic properties.

The thesis is structured as follows: in the section 2 the objectives of the work are mentioned. In the section 3 some concepts concerning to Rheology and Dysphagia are described, as well as information found in the literature about dysphagia diet food. The section 4 describes the materials and methods used in the experimental work. The results of the experimental work are presented and described in the section 5. Then a discussion of results is presented in the section 6. The conclusions of the work are in the section 7. Finally in the section 8 are mentioned some recommendations for future work.

2
Objectives

General objective

Evaluate the extensional viscosity of two pre-packed thickened foods, several thickened milk solutions and a contrast fluid with spoon-thick consistency in order to know the suitability of using these foodstuffs for dysphagic patients.

Specific objectives

- Measure the shear viscosity of a contrast fluid with spoon-thick consistency and two pre-packed thickened food.
- Measure the shear viscosity of thickened milks solutions, using two food thickeners, xanthan gum and citrus pectin, at different concentrations.
- Select the thickened milk solutions whose shear viscosity matches the one of the contrast fluid.
- Measure the extensional viscosity of the contrast fluid, pre-packed thickened foods, and selected thickened milk solutions using an orifice rheometer designed in the research group.
- Measure the stress relaxation modulus, elastic modulus and viscous modulus of the contrast fluid, pre-packed thickened foods, and selected thickened milk solutions.

3

Literature review

3.1 Rheology

3.1.1 Introduction

Throughout history human being has always sought to understand his environment. This has resulted in the generation of knowledge in many different fields. Knowledge of fluids is a field that has aroused great interest among scientists, especially since the knowledge gained is used in a wide range of applications.

In this sphere it is very important the work done by Robert Hooke. In 1678 he published a paper named “True Theory of Elasticity”, which explained the elastic behavior of the solids. Hooke proposed: "the power of any spring is in the same proportion with the voltage thereof".

Some years later, in 1687, Isaac Newton published *“Philosophiæ Naturalis Principia Mathematica”*. In this work he declared that the stress applied to a viscous fluid is directly proportional to the strain rate.

It was thought that Newton's law for viscous liquids and Hooke's law for elastic solids were sufficient to explain the behavior of any material. However, in the 19th century it was discovered that some materials exhibited both behaviors

simultaneously. As the two existing models could not explain the behavior of these materials it was clear the need to create a new area dedicated to understand this “unusual” behavior.

A Plasticity Symposium was held in 1929, where Eugene C. Bingham and M. Reiner named this area as Rheology (Doraiswamy, 2002). Rheology (from the Greek *reos*, meaning flow and *logos*, study) studies the flow and deformation of matter.

From a rheological standpoint, the matter can be subjected to two kinds of stresses: shear and extensional. The following sections describe the properties measured in each case.

3.1.2 Shear flow

When a substance flows its elements are deforming, and adjacent points in the substance are moving relative to each another. In the case of a shear flow, adjacent points move above each other in the same direction (Barnes, 2000), see Figure 3.1.

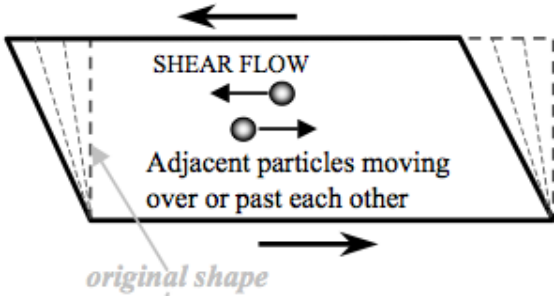

Figure 3.1. Particle motion in shear flow.

Adapted from: Barnes (2000).

To fully understand the shear flow consider two parallel plates and a material that is contained between them. The bottom plate remains fixed while the upper one is moving at speed V (Figure 3.2).

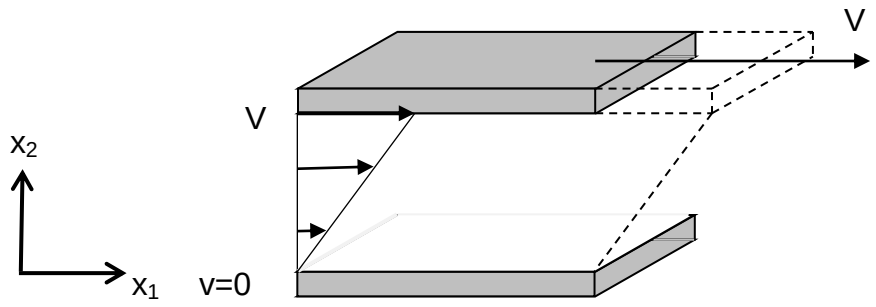

Figure 3.2. A material is contained between two plates, one is moving at a speed V.

Suppose the material moves like sheets, and that these do not mix between each other. Thus the velocity vector is:

$$\bar{u} = (\dot{\gamma} x_2, 0, 0) \tag{3.1}$$

where $\dot{\gamma}$ is the shear rate.

The velocity gradient tensor and the rate of deformation tensor are given, respectively, by:

$$\bar{\bar{\mathrm{L}}} = (\nabla \bar{u})^T = \begin{pmatrix} 0 & \dot{\gamma} & 0 \\ 0 & 0 & 0 \\ 0 & 0 & 0 \end{pmatrix} \tag{3.2}$$

$$2\bar{\bar{\mathrm{D}}} = (\nabla \bar{u})^T + \nabla \bar{u} = \begin{pmatrix} 0 & \dot{\gamma} & 0 \\ \dot{\gamma} & 0 & 0 \\ 0 & 0 & 0 \end{pmatrix} \tag{3.3}$$

The state of stress is described by the stress tensor $\bar{\bar{\mathrm{T}}} = -\mathrm{p}\bar{\bar{\mathrm{I}}} + \bar{\bar{\sigma}}$. The first term indicates the effect of the hydrostatic pressure and the second one describes all the effects of deformation.

Newtonian behavior

In the case of a Newtonian fluid $\overline{\overline{\sigma}} = \mu 2\overline{\overline{D}}$, thus:

$$\overline{\overline{T}} = -p\begin{pmatrix}1 & 0 & 0\\ 0 & 1 & 0\\ 0 & 0 & 1\end{pmatrix} + \mu\begin{pmatrix}0 & \dot{\gamma} & 0\\ \dot{\gamma} & 0 & 0\\ 0 & 0 & 0\end{pmatrix} \quad (3.4)$$

where μ is the shear viscosity.

In a Newtonian fluid the only stress generated is the shear stress and the shear viscosity does not vary with it.

$$T_{12} = \sigma_{12} = \mu\dot{\gamma} \quad (3.5)$$

Besides the viscosity is constant with respect the time of shearing, the stress in the liquid falls to zero immediately after the shearing is stopped (Barnes, Hutton, & Walters, 1989).

Non-Newtonian behavior

Non-Newtonian fluids are the ones whose behavior departs from the Newtonian behavior. That is the case of materials like dispersions, emulsions and polymer solutions. So the relationship between the shear stress and the velocity gradient ceases to be linear and the viscosity is a function of the shear rate.

$$\eta(\dot{\gamma}) = \frac{\sigma_{12}(\dot{\gamma})}{\dot{\gamma}} \quad (3.6)$$

Here, two typical examples of the non-Newtonian behavior are described (Figure 3.3):

(i) Shear-thickening behavior: it is also called “dilatancy”. The viscosity increases as the shear rate increases.
(ii) Shear-thinning behavior: it is also called “pseudoplasticity” and is the most common behavior. In the limit of very low shear rates (or stresses)

the viscosity is constant, whilst in the limit of high shear rates (or stresses) the viscosity is also constant but at a lower level, see Figure 3.4 (Barnes et al., 1989). Shear thinning is due to re-orientation, sorting, shape or aggregation of molecules or molecular aggregates when increasing shear stress.

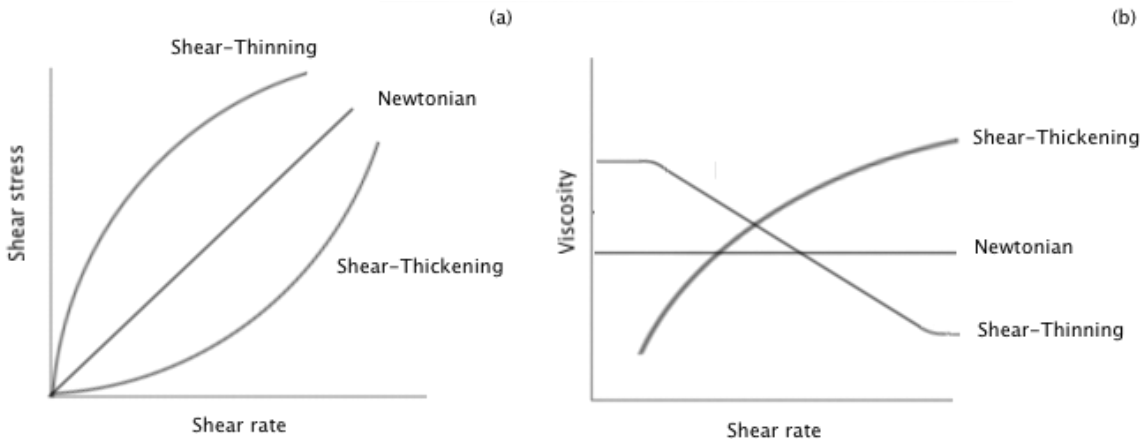

Figure 3.3. Typical behavior of a Newtonian fluid and non-Newtonian fluids.(a) Shear stress versus shear rate; (b) Viscosity versus shear rate.

Adapted from: Macosko and Larson (1994)

One of the mathematical models proposed to predict the shape of a general flow is the Cross model:

$$\eta = \eta_\infty + \frac{\eta_o - \eta_\infty}{1 + (K\dot{\gamma})^m} \tag{3.7}$$

Where η_o and η_∞ are the asymptotic values of the viscosity at very low and very high shear rates, respectively; K is a constant parameter with the dimension of time and m is a dimensionless constant. The Figure 3.4 shows a curve flow of a shear-thinning fluid.

If $\eta \ll \eta_o$ and $\eta \gg \eta_\infty$, thus $\eta_o \gg \eta_\infty$, the Cross model reduces to:

$$\eta = \frac{\eta_o}{(K\dot{\gamma})^m} \tag{3.8}$$

or equivalently

$$\eta = K_2\dot{\gamma}^{n-1} \tag{3.9}$$

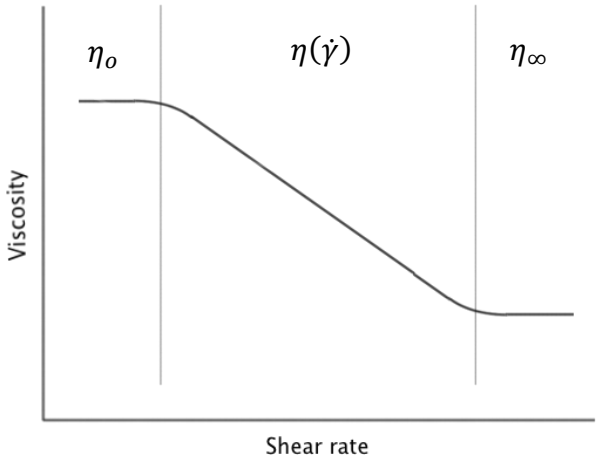

Figure 3.4. Viscosity function of a shear-thinning fluid.

The equation (3.9) is known as the “Power-law” model or the Ostwald-de-Waele model, where n is the power-law index (flow behavior index) and K_2 is an adjustment parameter.

Further, if $\eta \ll \eta_o$ in the Cross model, then:

$$\eta = \eta_\infty + \frac{\eta_o}{(K\dot{\gamma})^m} \tag{3.10}$$

which can be rewritten as

$$\eta = \eta_\infty + K_2\dot{\gamma}^{n-1} \tag{3.11}$$

The equation (3.11) corresponds to the Sisko model.

As can be seen in the Figure 3.5 these models cover different regions of the viscosity function.

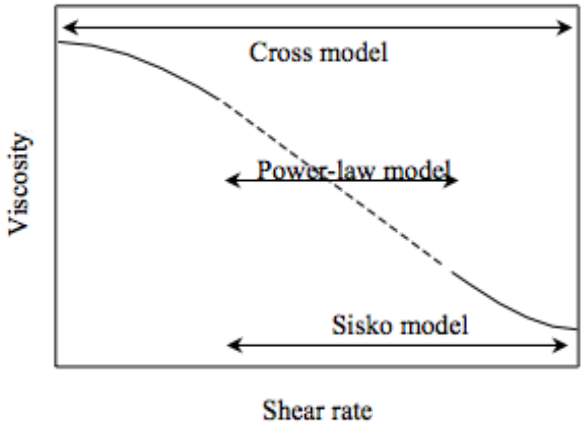

Figure 3.5. Diagram of the various models and the ranges they cover.

Adapted from: Barnes (2000)

3.1.3 Extensional flow

Although most rheological studies are carried out in simple shear flows, such as in rotational viscometers, flows are very often extensional (stretching or elongational) in nature (Figure 3.6), and for some fluids there can be a very large difference between their shear and extensional viscosities (Barnes, 2000).

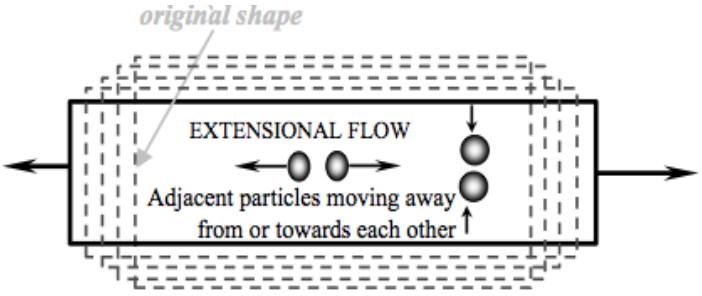

Figure 3.6. Particle motion in extensional flow.

Adapted from: Barnes (2000).

Consider an elastic material whose initial length is L_0 and is stretched to a length L. Thus a differential deformation is given by:

$$d\epsilon = \frac{dL}{L_0} \tag{3.12}$$

In the case of a liquid, a characteristic length L must be used instead of an initial deformation, so the differential deformation is given by:

$$d\epsilon = \frac{dL}{L} \tag{3.13}$$

Then the rate at which the fluid is deformed is:

$$\frac{d\epsilon}{dt} = \frac{1}{L}\frac{dL}{dt} = \dot{\epsilon} \tag{3.14}$$

where $\dot{\epsilon}$ is the extension rate.

But if the material is semi-solid, by integrating equation (3.13):

$$\int d\epsilon = \int \frac{dL}{L}$$

$$\epsilon_h = \mathrm{In}\left(\frac{L}{L_0}\right) \tag{3.15}$$

Equation (3.15) is known as the Hencky strain.

The extension rate will be constant if there is a homogeneous flow.

Suppose that an element is extended from position $x_1 = 0$ until x_1, then:

$$v_1 = \dot{\epsilon} x_1$$

In general:

$$v_1 = a_1 x_1 \tag{3.16}$$

$$v_2 = a_2 x_2 \tag{3.17}$$

$$v_3 = a_3 x_3 \tag{3.18}$$

The velocity gradient tensor is given by:

$$\bar{\bar{\mathrm{L}}} = (\nabla \bar{u})^T = \begin{pmatrix} \frac{\partial v_1}{\partial x_1} & 0 & 0 \\ 0 & \frac{\partial v_2}{\partial x_2} & 0 \\ 0 & 0 & \frac{\partial v_3}{\partial x_3} \end{pmatrix} \tag{3.19}$$

Substituting (3.16), (3.17) and (3.18) in (3.19):

$$(\nabla \bar{u})^T = \begin{pmatrix} a_1 & 0 & 0 \\ 0 & a_2 & 0 \\ 0 & 0 & a_3 \end{pmatrix} \tag{3.20}$$

The rate of deformation tensor is:

$$2\bar{\bar{\mathrm{D}}} = (\nabla \bar{u})^T + \nabla \bar{u} \tag{3.21}$$

Substituting (3.20) in (3.21):

$$2\bar{\bar{\mathrm{D}}} = \begin{pmatrix} 2a_1 & 0 & 0 \\ 0 & 2a_2 & 0 \\ 0 & 0 & 2a_3 \end{pmatrix} \tag{3.22}$$

Consider an incompressible material, the continuity equation is:

$$\frac{\partial v_1}{\partial x_1} + \frac{\partial v_2}{\partial x_2} + \frac{\partial v_3}{\partial x_3} = 0 \tag{3.23}$$

Substituting (3.16), (3.17) and (3.18) in (3.23):

$$a_1 + a_2 + a_3 = 0 \tag{3.24}$$

There are three basic types of extensional flow: uniaxial, biaxial and planar (Figure 3.7). Their corresponding rate of deformation tensor can be obtained using the equations (3.22) and (3.24) (Table 3.1).

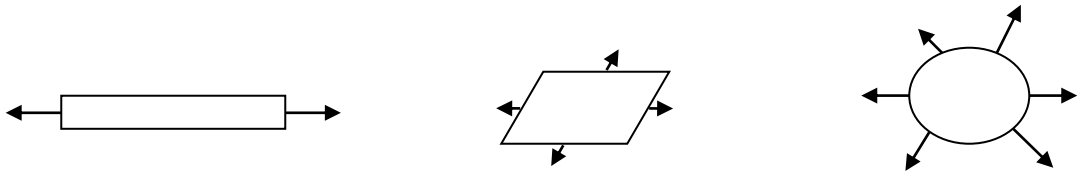

(a) (b) (c)

Figure 3.7. Schematic representation of uniaxial (a), biaxial (b) and planar (c) extension.
Adapted from: Chhabra and Richardson (2011)

Now consider a Newtonian fluid, with $\bar{\bar{\mathrm{T}}} = -\mathrm{p}\bar{\bar{\mathrm{I}}} + \mu 2\bar{\bar{\mathrm{D}}}$, then in the case of an uniaxial extension the stress tensor is:

$$\bar{\bar{\mathrm{T}}} = -p\begin{pmatrix} 1 & 0 & 0 \\ 0 & 1 & 0 \\ 0 & 0 & 1 \end{pmatrix} + 2\mu\dot{\epsilon}\begin{pmatrix} 1 & 0 & 0 \\ 0 & -1/2 & 0 \\ 0 & 0 & -1/2 \end{pmatrix} \tag{3.25}$$

By neglecting the effects of surface tension, the boundary conditions at the surface are:

$$T_{22} = T_{33} = 0 \tag{3.26}$$

Table 3.1. Basic extensional flows.

Flow	a_i	Rate of deformation tensor
Uniaxial	$a_1 = \dot{\epsilon}$ $a_2 = -\dot{\epsilon}/2$ $a_3 = -\dot{\epsilon}/2$	$2\bar{\bar{D}} = \dot{\epsilon}\begin{bmatrix} 2 & 0 & 0 \\ 0 & -1 & 0 \\ 0 & 0 & -1 \end{bmatrix}$
Biaxial	$a_1 = -2\dot{\epsilon}$ $a_2 = \dot{\epsilon}$ $a_3 = \dot{\epsilon}$	$2\bar{\bar{D}} = \dot{\epsilon}\begin{bmatrix} -4 & 0 & 0 \\ 0 & 2 & 0 \\ 0 & 0 & 2 \end{bmatrix}$
Planar	$a_1 = \dot{\epsilon}$ $a_2 = -\dot{\epsilon}$ $a_3 = 0$	$2\bar{\bar{D}} = \dot{\epsilon}\begin{bmatrix} 2 & 0 & 0 \\ 0 & -2 & 0 \\ 0 & 0 & 0 \end{bmatrix}$

Thus:

$$T_{11} = 3\mu\dot{\epsilon} \tag{3.27}$$

The extensional viscosity is defined as:

$$\mu_e = \frac{T_{11} - T_{22}}{\dot{\epsilon}} \tag{3.28}$$

Substituting (3.26) and (3.27) in (3.28):

$$\mu_e = 3\mu \tag{3.29}$$

Trouton (1906) and many later investigators found that, at low strain (or elongation rates), extensional viscosity was three times the shear viscosity (Barnes et al., 1989). The ratio μ_e/μ is referred to as the Trouton ratio (Tr) and thus:

$$Tr = \frac{\mu_e}{\mu} = 3 \tag{3.30}$$

The value of 3 for Trouton ratio for an incompressible Newtonian fluid applies to all values of shear and extension rates. By analogy, one may define the Trouton ratio for a non-Newtonian fluid:

$$Tr = \frac{\eta_e(\dot{\epsilon})}{\eta(\dot{\gamma})}$$

But this definition is ambiguous, since it depends on both $\dot{\epsilon}$ and $\dot{\gamma}$. To remove this ambiguity and at the same time provide a convenient estimate of viscoelastic effects it has been proposed the following definition, based on a simple analysis for an inelastic non-Newtonian fluid (Barnes et al., 1989):

$$Tr(\dot{\epsilon}) = \frac{\eta_e(\dot{\epsilon})}{\eta(\bar{\gamma})}$$

where $\bar{\gamma}$ is the effective strain rate defined by (Morrison, 2001):

$$\bar{\gamma} = \left|2\bar{\bar{\mathrm{D}}}\right|$$

$$\bar{\gamma} = +\sqrt{\frac{1}{2}\begin{pmatrix} 2\dot{\epsilon} & 0 & 0 \\ 0 & -1\dot{\epsilon} & 0 \\ 0 & 0 & -1\dot{\epsilon} \end{pmatrix} : \begin{pmatrix} 2\dot{\epsilon} & 0 & 0 \\ 0 & -1\dot{\epsilon} & 0 \\ 0 & 0 & -1\dot{\epsilon} \end{pmatrix}}$$

$$\bar{\gamma} = +\sqrt{\frac{1}{2}(4\dot{\epsilon}^2 + \dot{\epsilon}^2 + \dot{\epsilon}^2)} = \sqrt{3}\dot{\epsilon}$$

Extensional thinning

When a fluid is subjected to an extensional flow it may occur that the extensional viscosity decreases with increasing the extension rate. Barnes (2000) offers the following explanation for this phenomenon:

Consider a Newtonian liquid with a high concentration of fibres. Because of this there are many contacts between individual fibres, and the number of these contacts dominates the viscosity. In a polymer solution or melt these contacts are intermolecular entanglements.

At rest the transient network formed as the fibres or chains become entangled and disentangled under the action of Brownian motion, and stretching strongly interferes with the dynamics of this transient network. If the inverse of the extension rate is greater than the average lifetime of the entanglements forming the network, then momentarily the polymer segment between two entanglements is acting as part of an elastic solid, and the stress increases considerably, until the entanglements would rupture. If, in this situation, the average number of entanglements is constant, then it can be shown that the extensional viscosity increases dramatically with extension rate while the shear viscosity remains constant. However, in reality, as the deformation rate increases, the number of entanglements (and possibly their lifetime) begins to decrease with increasing extension rate, then the viscosity, after increasing, drops again, and at the same point the shear viscosity also begins to fall. The overall effect is shown in Figure 3.8.

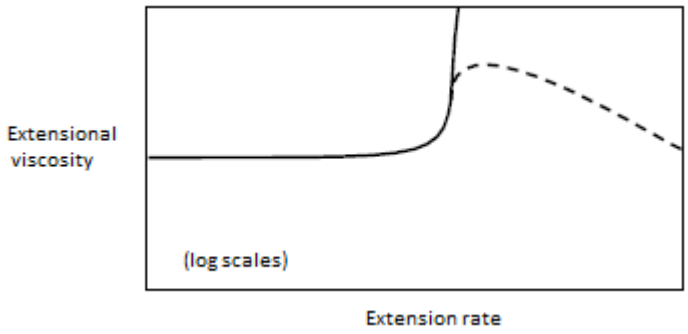

Figure 3.8. Extensional viscosity of a polymer network. Network dynamics effects shown as solid lines, and the effect of loss of junctions shown as dotted lines.

Adapted from: Barnes (2000)

In the literature there are some examples of this behavior. Such is the case of Różańska et al., (2013), who measured the extensional viscosity of mineral oil-in-water emulsions. The Figure 3.9 shows the dependence of the extensional viscosity on extension rate for emulsions stabilized by the addition of xanthan gum. Decreased extensional viscosity in emulsion with increment of strain rate

can be explained, in this case, by disintegration of aggregates composed of emulsion droplets.

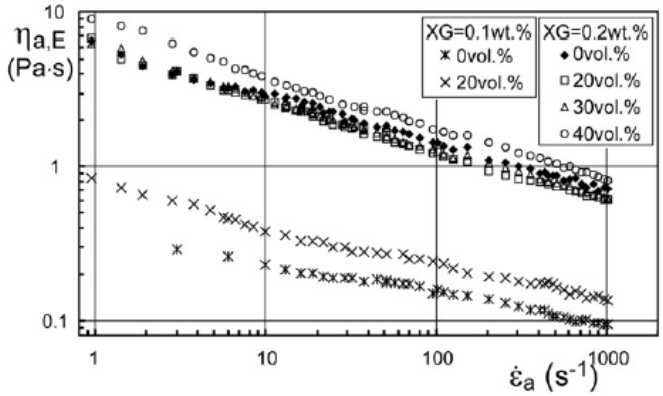

Figure 3.9. Extensional viscosity as a function of extension rate for emulsion stabilized with xanthan gum.

Adapted from: Różańska et al., (2013)

Tan, Tam, Tirtaatmadja, Jenkins, and Bassett (2000) studied the extensional viscosity of a series of model hydrophobically modified alkali-soluble associative (HASE) polymers. The extensional viscosity of one of them is shown in the Figure 3.10. It can be seen that as the extension rate is increased further, the extensional viscosity exhibits a decline, possibly due to the disruption of the inter-molecular junctions and the subsequent alignment of polymer backbones.

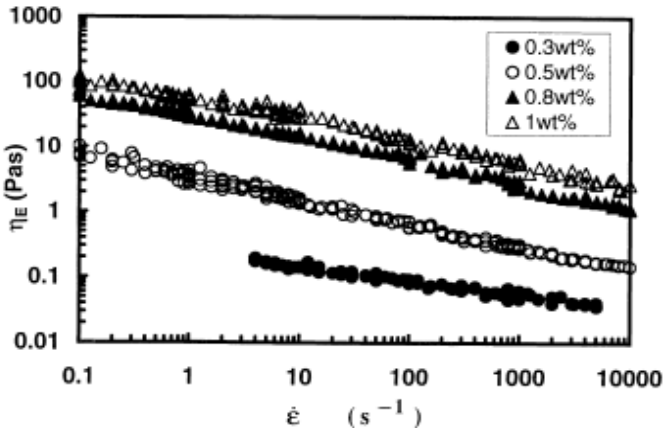

Figure 3.10. Extensional viscosity as a function of extension rate for a model HASE polymer at various polymer concentrations.

Adapted from: Tan et al. (2000)

Experimental techniques

Experimental techniques for measuring the extensional viscosity are not so developed as those for measuring the shear viscosity. This lack of development is due to it has been complicated generate in the laboratory pure extensional flows (Chen, 2009).

One of the simplest techniques to determine the extensional properties of low viscosity liquids or suspensions is the pressure entrance flow method, which consists of running a flow through a contraction. This causes a pressure drop as result of friction on the wall surface, extensional deformations in the flow center and changes in kinetic energy (Macosko & Larson, 1994; Valle, Tanguy, & Carreau, 2000).

Using a contraction generates an uniaxial extensional flow, where a strong stretch occurs in the flow direction and contraction occurs equally in the other two directions (Morrison, 2001).

Abrupt contractions have been used in some studies, but they have generated vortex and stagnation zones, which affects final results (Ascanio, Carreau, Brito-de la Fuente, & Tanguy, 2002; Muñoz-Díaz, Solorio-Ordaz, & Ascanio, 2012). The use of an orifice rheometer with an axisymmetric contraction, as developed by Naranjo (2010), has been recommended to avoid some of these problems. Because of this, several researchers have measured extensional properties with profiled contractions. For example Stading (2008) measured the extensional viscosity for wheat and sorghum doughs using a hyperbolic contraction, see Figure 3.11.

In this work a semihyperbolic contraction, designed by Muñoz-Díaz (2012), was used.

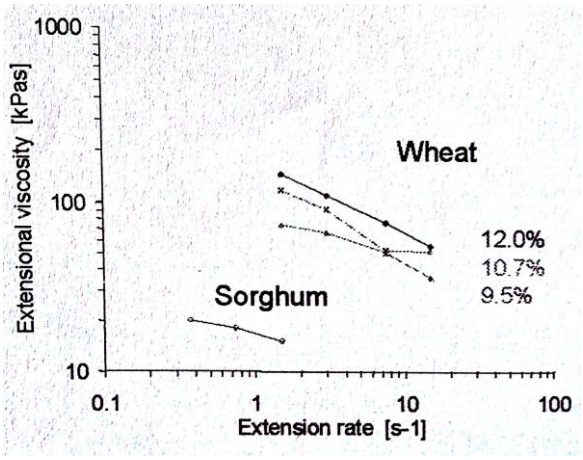

Figure 3.11. Flow curves for wheat and sorghum doughs. The protein content of the wheat flour is given in the figure.

Adapted from: Stading (2008).

3.1.4 Viscoelasticity

As mentioned above there are a lot of materials having characteristics of both elastic solid and viscous fluid. The deformation produced on an elastic solid is proportional to the force applied, and when this ceases the elastic solid returns to its original state. In a viscous fluid the strain rate is proportional to the applied force. In this case when the force is stopped the fluid is unable to recover its original state because the mechanical energy supplied has been dissipated completely. Hence a viscoelastic material is one that shows characteristics of elastic solid and viscous fluid. This means that a part of the energy supplied is stored in the material and the other part is dissipated.

The viscoelastic properties depend on the time of observation of the experiment. If it is too long, the material may seem more viscous than elastic, but if it is short, the material may seem more elastic than viscous. Then an intermediate time of observation will let us see both elastic and viscous properties.

The magnitude of the applied deformation (or stress) also has an important role in the response of the material. If a material is submitted to deformations or

stresses small enough, so that its rheological functions do not depend on the value of the deformation or stress, the material response is said to be in the linear viscoelasticity range (Gallegos & Martínez-Boza, 2010).

Characterization of viscoelastic fluids

There are two types of methods to study the linear viscoelastic behavior: static and dynamic. Static tests involve the imposition of a step change in stress (or strain) and the observation of the subsequent development in time of the strain (or stress). Dynamic tests involve the application of a harmonically varying strain (Barnes et al., 1989).

The tests used in this work are described below:

- **Small-amplitude oscillatory shear test**

This is a dynamic type experiment. In this case a sinusoidal strain is applied to the material. The strain varies with time according to the next expression:

$$\gamma = \gamma_0 \sin(\omega t) \tag{3.31}$$

where γ_0 is the strain amplitude and ω is the frequency. The stress varies with the same frequency, but showing an offset δ from the strain.

$$\sigma = \sigma_0 \sin(\omega t + \delta) \tag{3.32}$$

where σ_0 is the stress amplitude.

The strain can be decomposed into two parts, one in phase with the strain (σ') and the other 90° phase shift (σ'').

$$\sigma = \sigma' + \sigma'' \tag{3.33}$$

From (3.33) is defined a modulus associated with the elastic energy of the material (G', elastic modulus) and a modulus associated with the viscous energy (G'', viscous modulus). They are defined by the following equations:

$$G' = \frac{\sigma_0'}{\gamma_0} \qquad\qquad G'' = \frac{\sigma_0''}{\gamma_0}$$

It is possible to relate G' and G'' with δ by the equation

$$\tan\delta = \frac{G''}{G'} \tag{3.34}$$

In an elastic material the stress and the strain are in phase (δ = 0º), while in a viscous material the stress and strain are offset (δ = 90º), see Figure 3.12. Then, in a viscoelastic material δ will have values between 0º and 90º.

The behavior of the elastic and viscous moduli provides information about the polymer structures on food hydrocolloids (Nishinari, 2000):

(i) For a strong gel (an elastic gel or a true one), G' is far larger than G'', and both moduli G' and G'' are independent of frequency.

(ii) For a weak gel, G' is slightly larger than G'', and the two moduli are only slightly dependent on frequency.

(iii) In the case of a true polymer solution, G' is smaller than G'' at lower frequencies, but both moduli G' and G'' increase with increasing frequency and show a crossover, G' becoming larger than G'' at higher frequencies.

(iv) For a dilute polymer solution, G' is far smaller than G'' at all frequencies, and both moduli G' and G'' are strongly dependent on the frequency, and at very low frequencies the relations $G' \sim \omega^2$ (the slope of $\log_{10} G'$ *vs.* $\log_{10}\omega$ plot is 2) and $G'' \sim \omega$ (the slope of $\log_{10} G'$ *vs.* $\log_{10}\omega$ plot is 1) are known.

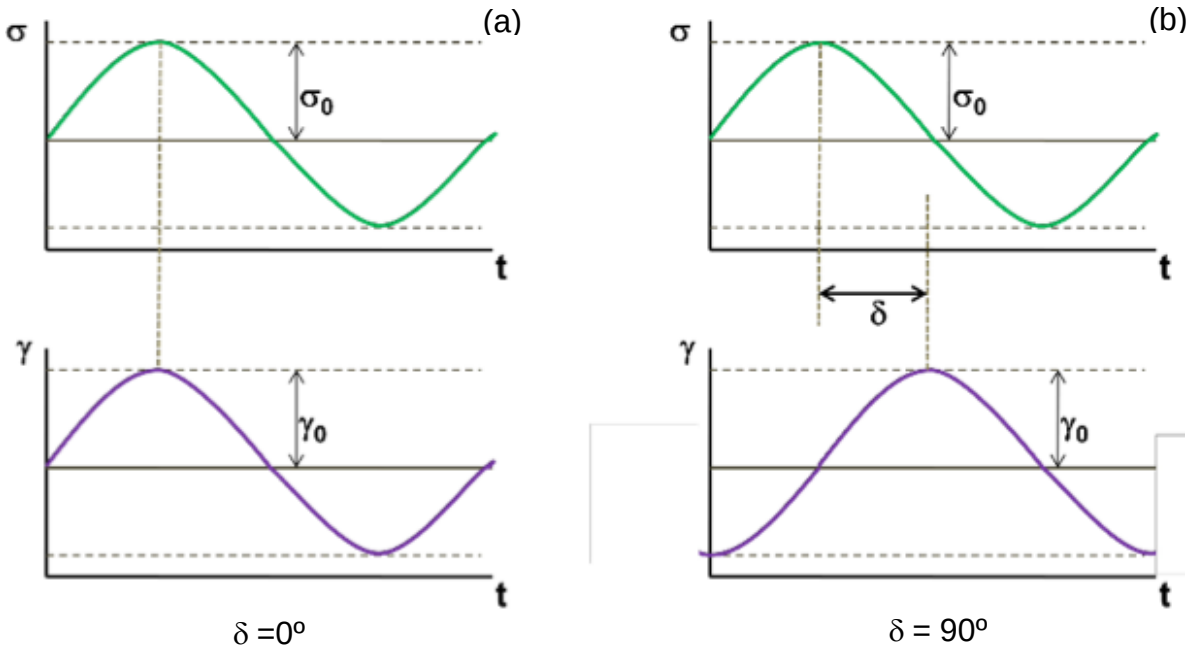

Figure 3.12. Outcome from small-amplitude oscillatory shear test: (a) elastic material, (b) viscous material.

Also there are the following relationships:

$$\sigma_0 = |G^*|\gamma_0 \tag{3.35}$$

$$|G^*| = \sqrt{G'^2 + G''^2} \tag{3.36}$$

where G^* is the complex modulus.

Another variable used is the complex viscosity η^*. The equation (3.37) shows the relationship between some of the variables studied so far:

$$\eta^* = \frac{G^*}{\omega} = \eta' - i\eta'' \tag{3.37}$$

where η' and η'' are given by:

$$\eta' = \frac{G''}{\omega} \qquad\qquad \eta'' = \frac{G'}{\omega}$$

These functions also give an idea of the viscous and elastic character of the material, and as G' and G'', they are frequency dependent parameters.

Several investigations on the rheological properties of polymer solutions have shown that there is a correlation between the functions describing the dynamic properties and those characterizing the properties in steady-shear flow (Lopes da Silva, Gonçalves, & Rao, 1993).

Cox and Merz (1958) observed that the complex viscosity is nearly equal to the steady-shear viscosity when the shear rate and frequency are equal:

$$\eta(\dot{\gamma}) = |\eta^*(\omega)| \; ; \qquad \text{at } \omega = \dot{\gamma}$$

as long as the structure that determines the mechanical properties of the material remains intact under steady flow (Ikeda & Nishinari, 2001). This relationship often holds fairly well at high shear rates (Macosko & Larson, 1994).

This empirical relationship, now referred to as the “Cox-Merz rule” may be useful for materials that are more easily tested under oscillatory instead of steady shear conditions (Steffe, 1996).

- **Stress relaxation**

In this test, a constant strain is applied instantaneously to the sample and the stress is measured on time (static test). A Hookean solid shows no stress relaxation, a Newtonian fluid relaxes as soon as strain is constant, while a viscoelastic solid or liquid would relax gradually over a period of time (Figure 3.13). In the case of a viscoelastic liquid stress relaxes to zero, while for a viscoelastic solid this approaches asymptotically a steady stress.

The relaxation of shear stress σ after a step shear strain γ from rest can be expressed in terms of relaxation modulus function:

$$G_s(\gamma, t) = \frac{\sigma(\gamma, t)}{\gamma} \tag{3.38}$$

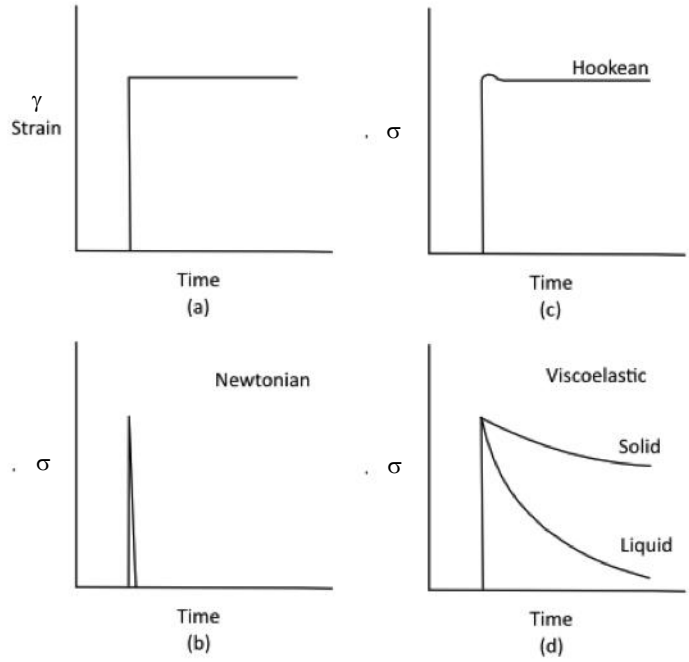

Figure 3.13. Stress response versus time for a step input strain: (a) Hookean solid, (b) Newtonian fluid and (c) viscoelastic liquid or solid.

Adapted from: Macosko and Larson (1994).

Experimental measurements have shown that beyond a certain time (depending on the system), the modulus function can be expressed in a factored form:

$$G_s(\gamma, t) = h(\gamma)G(t) \tag{3. 39}$$

where h is the function damping. It is a monotonically decreasing function of strain (Vrentas & Graessley, 1982). The damping function gives valuable

information regarding the microstructural breakdown process of a material under increasing deformations, outside linear viscoelasticity region (Quinchia et al., 2011).

In the limit of small strain $G_s(\gamma, t)$ becomes $G(t)$, the shear stress relaxation modulus of linear viscoelasticity (Vrentas & Graessley, 1982). Knowledge of the evolution of the linear relaxation modulus with time is essential to model the nonlinear viscoelastic behavior of complex fluids (Brito-de la Fuente, Ekberg, & Gallegos, 2012).

3.2 Dysphagia

3.2.1 Introduction

Taking food into the mouth, chewing and swallowing it, and then to continue its way up to the stomach is a fundamental process to provide nutriments to the organism. Swallowing process is particularly important.

A variety of diseases (stroke, brain injury, amyotrophic lateral sclerosis, Parkinson's disease, etc.), may cause disorders in the swallowing process, although they can also appear as a medical treatment side effect (radiation therapy or surgery for head and neck cancer)(García-Peris & Parón, 2007; Stegemann, Gosch, & Breitkreutz, 2012). This kind of disorders that affect or impair swallowing is clinically known as dysphagia. Patients with dysphagia have difficulty to swallow solid food, semisolid food and/or liquids (Groher, 1997; Whelan, 2001).

3.2.2 Swallowing phases

Swallowing process involves several structures and body regions. The entire process begins in the oral cavity, then continues in the pharynx, and ends in the esophagus (Figure 3.14).The process has been divided into several phases in order to have a better understanding of it, see Figure 3.15. These phases are

described below (Buettner, Beer, Hannig, & Settles, 2001; Garcia & Chambers, 2010; Logemann, 2007; Stegemann et al., 2012):

(i) Oral phase: food is chewed and mixed with the saliva to get a homogeneous bolus. Then the tongue moves the bolus toward the back of the oral cavity. Since the tongue is made entirely of muscle it is able to apply variable pressure on the tail of the bolus. The amount of pressure needed during a swallow increases sequentially as the bolus becomes thicker. Finally several receptors are stimulated and the swallowing response is triggered.

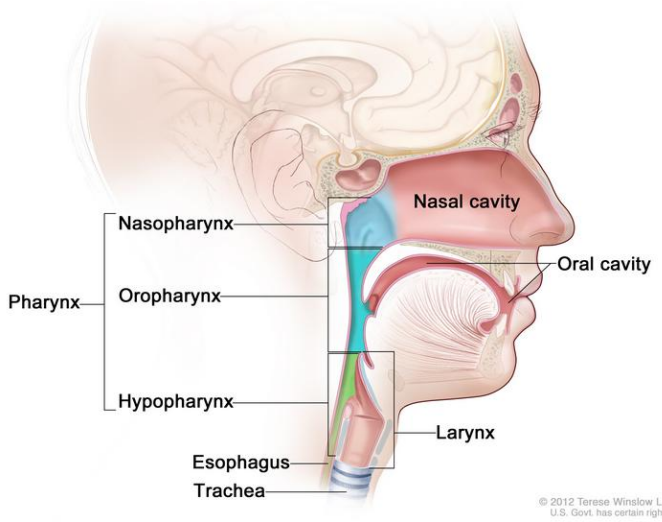

Figure 3.14. Regions of the human body involved in swallowing.

(ii) Pharyngeal phase: a complex interaction of events takes place in this phase for moving the bolus from the pharynx towards the esophagus. To understand better this phase it is important to know the role played by three valves located in the oropharyngeal region.

The first one is the velopharyngeal valve. It is responsible for closing the nasal cavity in order to prevent the entry of the bolus. If the velopharyngeal closure is inadequate the pressure needed to propel the

bolus through the pharynx will be inadequate, leaving a great deal of residue in the pharynx after the swallow.

The second valve is the pharynx. It must be closed to prevent the bolus goes into the airways. If something enters in the pharynx a reflexive cough will occur to expel it.

And the third valve is the base of tongue that must make contact with the posterior pharyngeal wall during all swallows. This valve drives the bolus through the pharynx by generating needed pressure.

So, when the swallowing reflex is triggered the following events occur: the breathing is stopped; the nasal cavity and the larynx are closed and the walls of the pharynx begin to contract to propel the bolus through the pharynx. Finally, the upper esophageal sphincter opens, so the bolus passes into the esophagus.

(iii) *Esophageal phase*: the bolus is moved toward the stomach by an involuntary wave or contraction.

Swallowing is considered as a complex process because at least 25 pairs of muscles are involved, and all of them move in a synchronized way for the process be successful (Hiiemae, 2004).

3.2.3 Types of Dysphagia

Dysphagia has been classified as a function of the region in which complications arise. Below two types of dysphagia are described (Garcia & Chambers, 2010; Nazar, Ortega, & Fuentealba, 2009):

(i) *Oropharyngeal*: transferring the bolus or the liquids towards the esophagus is difficult and risky. Characteristics of oropharyngeal dysphagia are excessive salivation, delay to start swallowing, nasal regurgitation, coughing with swallowing (possibly with feeling of choking), repeated swallows, etc. Some of the causes of oropharyngeal dysphagia are: the function of the tongue may be impaired, an absence or delay of

the swallowing response, an impaired peristalsis, an incorrect closure of the nasal passages, among others.

(ii) Esophageal: there are problems to transfer adequately the bolus to the stomach. The patient may have a sensation of obstruction, chest pain and regurgitation.

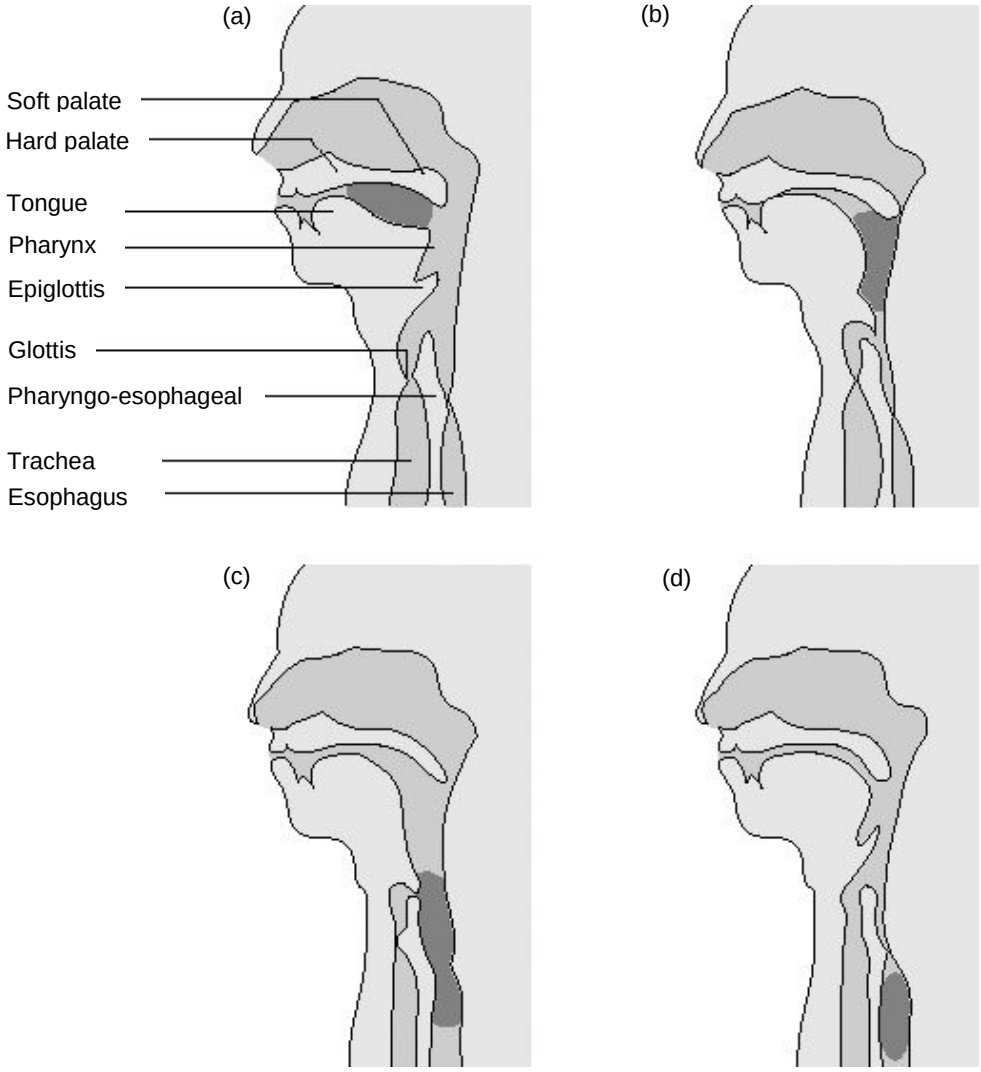

Figure 13.11. Movement of food bolus (black) during swallowing.

Adapted from: (Linden, 1998).

Dysphagia is also classified as mechanical and motor. Mechanical dysphagia is caused by a large bolus and a narrow diameter of the swallowing passage. Dysphagia due to weakness of peristaltic contractions or to impaired deglutitive inhibition causing non-peristaltic contractions and impaired sphincter relaxation is called motor dysphagia (Fauci, Braunwald, & Fuselbacher, 1998).

3.2.4 Aspiration

The speed of the bolus, according to several researches, is affected by its rheology and the stage of the swallowing. It has been observed that the maximum speed is reached in the pharyngeal stage, where a reconfiguration is performed to protect the airways and open the way to the stomach. When a subject is unable to make these changes in time, it may happen that the bolus is pushed into the pharynx while the airway is still open and then, aspiration occurs. It has also been found out that the speed of the bolus and the risk of aspiration decrease by increasing the shear viscosity of the bolus, because if the bolus flows slower, the pharynx has more time to close the airways and so the aspiration is avoided (Brito-de la Fuente et al., 2012; Germain, Dufresne, & Ramaswamy, 2006).

3.2.5 Diagnosis

In most instances, a number of professionals interact to define the diagnosis and treatment plan for the patient. Diagnosing involves a clinical assessment followed by instrumental measures (videofluoroscopy, ultrasound, fibre-optic endoscopic**,** scintigraphic, etc.) (Logemann, 2007).

Examinations with any instrumental technique aim to identify the exact nature of the swallowing disorder. It has been reported that using these techniques increases the chances for detecting and properly diagnosing dysphagia (Coster & Schwarz, 1987; Martino et al., 2005). Also, these techniques have been used in several researches to know the relationship between swallowing and bolus properties (Clavé et al., 2006; Ekberg, Olsson, & Sundgren-Borgstrom, 1988; Groher, Crary, Carnaby, Vickers, & Aguilar, 2006; Hamlet et al., 1996).

Videofluoroscopy examination is one of the most used methods for diagnosing dysphagia. It allows to observe in real time the bolus behavior during swallowing and thus determine the patient's particular situation (Chen et al., 1992; Leder & Murray, 2008; Logemann, 2007).The information obtained is useful since apparently the risk of aspiration of food depends mainly on the patient (Ozaki et al., 2010).

In the videofluoroscopy test the patient ingests small amounts of a radiopaque material and then the bolus transit is observed by X-rays (Figure 3.16). This procedure is repeated with different viscosities, thus it is possible to know which of them are safe for the patient. The radiopaque material used is barium sulfate, which is biologically inert.

3.2.6 Management

Once the patient has been diagnosed, the next step is to develop a treatment plan. Treatment generally includes behavioral intervention (postural changes, exercise programs, etc.), changes in diet, and sometimes surgical interventions (Logemann, 2007).

Figure 3.16. Videofluoroscopy image (side vision). The image shows the bolus transit trough the pharynx and upper esophagus.

Adapted from: Nazar et al. (2009)

3.3 Dysphagia diet food

3.3.1 Introduction

Patients with dysphagia should be very careful about their diet. Hence the outcome of the diagnosis is useful because it helps to know the features that will make a food safe. Thus, patients are able to eat without any risk and obtain the nutrients needed for a good health.

Therapist aims to provide food whose features are as close as possible to those of the contrast fluid that resulted safe during the diagnosis. Commonly the food is thickened until the viscosity reaches the contrast fluid's viscosity (Chen et al., 1992). It seems that this increasing has a positive influence on the patients likely because increasing the viscosity decreases the speed at which the bolus is moved (Chen, 2009; Meng, Rao, & Datta, 2005).

Several researchers have proposed explanations about how the swallowing becomes safer with a higher viscosity. Below some of these are listed:

- The oral cavity is not sealed

  During the oral phase the oral cavity is not sealed and then the bolus may spill into the pharynx when the swallowing reflex has not been triggered yet. This is less likely to occur if the bolus has a high viscosity due to the bolus would have more difficulty to flow through an opening so small (Coster & Schwarz, 1987).

- The bolus reaches the pharynx before the airways are closed.

  A decrease in the speed of the bolus, by a high viscosity, would yield more time for closing the airways (Brito-de la Fuente et al., 2012).

- The airways are opened before the bolus is expelled from the pharynx.

It is believed that a high viscosity could increase the propulsive force of the tongue and pharynx, which would cause the bolus be evacuated before the airways be opened (Raut, McKee, & Johnston, 2001).

There is a grading system proposed by the American Dietetic Association (ADA), which aims to establish standard labels and ranges for liquids at 25 ºC and 50 s^{-1} (Table 3.2). Some therapists use this grading system as a reference for preparing foods with different levels of viscosity for their patients. However, this has been criticized because the ADA does not clarify why 50 s^{-1} and 25 ºC have been chosen. Besides during the swallowing process the bolus is subjected to different shear rates (Brito-de la Fuente et al., 2012). Hence it is not a suitable system.

Table 3.2. Proposed terms and viscosity ranges for dysphagia diet food.

Liquid	Viscosity range (cP)
Thin	1-50
Nectar-like	51-350
Honey-like	351-1750
Spoon-thick	>1750

From the National Dysphagia Diet Task Force

3.3.2 Thickeners

Food thickening is made with thickeners. These substances belong to a group of polysaccharides known as hydrocolloids. Hydrocolloids are high molecular weight polysaccharides whose main feature is their ability for binding water. This feature allows increasing viscosity to the desired level.

There are a large number of thickeners the most of them are based on gums, starches and citrus pectin. And although all of them form networks where water is trapped, there are some differences. For example, Matta, Chambers, Mertz and McGowan (2006) made a study to compare the effect of gums and starches

on beverages. They found that using gums the viscosity was more consistent regardless of the type of beverage.

Thickeners based on starch are widely used. However, they produce a viscosity that varies in time, which is a great disadvantage. This was observed by Garcia, Chambers, Matta and Clark (2008) when they prepared thickened beverages using thickeners based on starch and xanthan gum. In the first 30 minutes beverages with xanthan gum maintained its viscosity while beverages with starch increased it. Payne, Methven, Fairfield and Bell (2011) made a research using pre-thickened food based on starch. They found that viscosity was different from that indicated on the package. It is believed that this variation is due to the continued hydration of starch network.

Others thickeners too show this kind of problems. Dewar and Joyce (2006) found that the viscosity produced by a starch-based thickener continued decreasing after four hours of being prepared. They also measured the viscosity produced by a maltodextrin-based thickener, but in this case the viscosity increased dramatically during the first 2 hours.

Commercial thickening agents have manufacturer's indications about the amount needed to achieve a certain viscosity; however these amounts are not specific for a dispersing medium. Several studies have shown that the dispersing medium plays an important role in the viscosity obtained (Sopade et al., 2008; Sopade, Halley, Cichero, & Ward, 2007). Such is the case of orange juice which components may enhance the bonding characteristics of the thickener what results in more significant thickening over time (Garcia et al., 2008).

3.3.3 Dysphagia food preparation

In hospitals the dysphagia diet food is prepared by the staff, nevertheless they use a subjective judgment to choose the amount of thickener added to each food. The outcome is that the final viscosity depends mainly on the subject who

prepares the food (Goulding & Bakheit, 2000; Steele, Van Lieshout, & Goff, 2003).

Food prepared in this way is a risk for patients since its viscosity is not matched with the viscosity declared as safe in the diagnosis. Cichero, Hons, Jackson, Halley and Murdoch (2000) studied in a hospital the mealtime fluids and their allegedly matched videofluoroscopy counterparts, all of them prepared by the staff. The results showed a poor correlation between them for all the parameters analyzed. A similar situation happened between a commercial fluid contrast and a thickened infant formula (Stuart & Motz, 2009).

Although it may be thought that a higher viscosity than necessary would cause no problem it has been reported that a higher viscosity causes a decline in the amount of food eaten. This lead dehydration and reduced calorie intake in these patients (Goulding & Bakheit, 2000).

3.3.4 Rheology

In the literature there are a great number of researches about the shear viscosity of dysphagia food. They report a shear-thinning behavior in all the cases (Claes et al., 2012; Dewar & Joyce, 2006; Germain et al., 2006; Leder, Judson, Sliwinski, & Madson, 2012; O'Leary, Hanson, & Smith, 2010; Popa, Murith, Chisholm, & Engmann, 2013; Sopade et al., 2008, 2007). This kind of behavior is to be expected because dysphagia food contains complex carbohydrates as thickeners (Strowd, Kyzima, Pillsbury, Valley, & Rubin, 2008).

Other properties too have been measured, as the viscoelasticity. Wendin et al. (2010) characterized 15 products and they all were more elastic than viscous. In another research a total of 34 commercial enteral nutrition products were analyzed, their behavior was predominantly more elastic than viscous (Casanovas, Hernández, Martí-Bonmatí, & Dolz, 2011). Other researches have reported a gel-like behavior in this kind of products (Claes et al., 2012; Seo & Yoo, 2013).

Instrumentals techniques have been used for measuring the velocity in the swallowing process. The results show that the velocity of the bolus is different in each phase and reaches the maximum velocity in the pharyngeal phase (Bardan, Kern, Arndorfer, Hofman, & Shaker, 2006; Nguyen, Silny, & Albers, 1997; Omari et al., 2006). Brito-de la Fuente et al. (2012), under the assumption that bolus deformation only occurs in shear, used these data to make an estimation of the shear rates. They found that the shear rate spectrum for the whole swallowing process goes from 1 to 1000 s^{-1}.

However pictures of videofluoroscopy and real-time magnetic resonance imaging show clearly how the bolus is extensively stretched during swallowing. Thus the deformation of food bolus is expected to be not only in shear but also in elongational (Chen, 2009).

The importance of the extensional viscosity is clear if we look at the swallowing process. The bolus flows from the mouth into the open pharynx, passes a relatively narrow part and reaches the wider esophagus. When the bolus passes the narrow part it is forced to extend and the extensional viscosity plays a more important role than the shear viscosity. Besides in the mouth the bolus is squeezed between the tongue and the pallet, which also causes a mainly extensional flow (Stading et al., 2007).

The pressure drop is the driving force for bolus flow and deformation between the oral cavity and the pharynx. Taking into account that a pressure of 10 kPa would normally be applied in the oral cavity but a pressure of about 4 kPa in the pharynx (Ferguson, Shuttleworth, & Whittaker, 1999) then a pressure drop of around 6 kPa will be used to overcome the friction energy loss during bolus movements and the fluid resistance against flow deformation. Because of the saliva incorporation and highly lubricated oral surfaces, it is reasonable to believe that the friction loss should be relatively small and less significant. The major energy consumption (or pressure drop) would mostly likely to be caused by the stretching deformation of the food bolus during oropharyngeal transition (Chen & Lolivret, 2011).

Chen (2009) made an estimation of the extension rate in the swallowing process. He used experimental data from Hasegawa, Otoguro, Kumagai and Nakazawa (2005) (a bolus of 15 ml being swallowed at a speed of 0.5 m/s and a transit time of 1 s) and obtained that the bolus could be extensionally stretched at a rate of around 1 s^{-1}.

A research made by Stading et al. (2007) showed that the extensional viscosity affects in a significant way the sensory perception. They mixed barium sulfate with mango purée and found that increasing the concentration of barium sulfate caused an increase in the extensional viscosity, while the shear viscosity hardly changed, see Figure 3.17. Sensory analysis showed that addition of barium sulfate makes the mixture considerably more difficult to swallow (Ekberg et al., 2009).

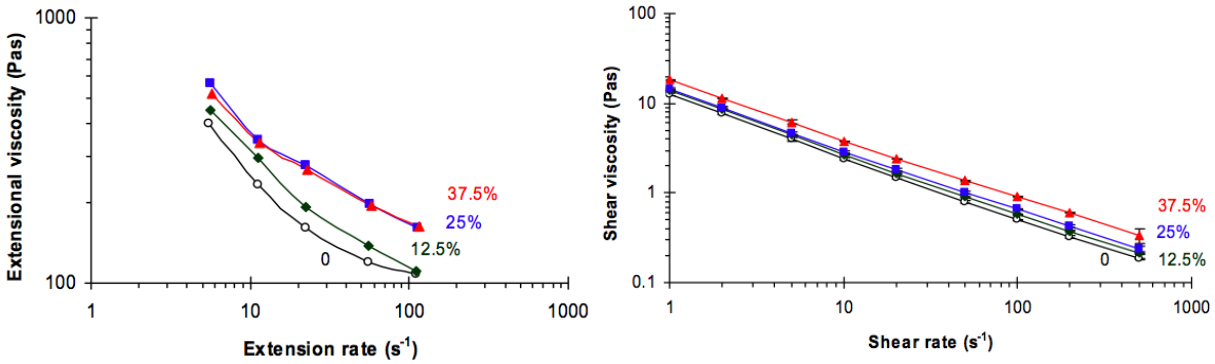

Figure 3.17. Mango purée with barium sulphate. a) Extensional viscosity, b) Share viscosity.

Adapted from: Stading et al. (2007)

Wendin et al., (2010) characterized about 15 food samples by descriptive sensory and rheological measurements. They found a strong correlation between perceived ease of swallow and extensional viscosity. Chen and Lolivret (2011) studied a wide range of fluid foods. They believe that extensional property could be the key determining factor in triggering a swallowing.

4

Materials and methods

4.1 Materials

4.1.1 Barium sulfate suspension (BSS)

The videofluoroscopic contrast fluid chosen in this work is a commercial barium sulphate suspension (Varibar® Pudding with spoon-thick consistency) from E-Z-EM, Inc, Lake Success, NY. Each 100 mL contains 40 g barium sulfate. Other ingredients are: artificial vanilla flavor, citric acid, carboxymethylcellulose sodium, ethyl vanillin, glycerin, maltodextrin, natural gum, polysorbate 80, potassium, purified water, saccharin sodium, simethicone emulsion, sodium benzoate, and xylitol.

4.1.2 Pre-packed thickened food

Two proprietary pre-packed thickened formulations from Fresenius-Kabi Deutschland GmbH were selected. It was reported by Brito-de la Fuente, Quinchia, and Valencia (2010) that these products match their rheological properties in shear with the Varibar® Pudding spoon-thick consistency. Below the ingredients of each product are mentioned:

Strawberry pudding. Water, sucrose, whey protein, fermented skimmed milk powder, vegetable oils, modified starch, acidity regulator (E 270), calcium lactate, maltodextrin, thickener (E 440), emulsifiers (soya lecithin, E 471), flavourings, choline hydrogen tartrate, vitamin C, sodium chloride, iron pyrophosphate, zinc sulphate, colouring (E 120), magnesium oxide, niacin, vitamin E, pantothenic acid, manganese chloride, copper sulphate, vitamin B_2, vitamin B_6, sodium fluoride, vitamin A, vitamin B_1, folic acid, chromium chloride, sodium selenite, potassium iodide, sodium molybdate, vitamin K_1, biotin, vitamin D_3, vitamin B_{12}.

Vanilla pudding. Water, sucrose, milk protein, vegetable oils, maltodextrin, inulin, thickeners (E 1442, E 440), potassium citrate, flavoring, emulsifiers (soya lecithin, E 471), vitamin C, sodium citrate, sodium chloride, magnesium oxide, magnesium citrate, iron pyrophosfate, zinc sulfate, niacin, manganese chloride, pantothenic acid, vitamin E, copper sulphate, vitamin B_2, vitamin B_6, sodium fluoride, vitamin B_1,carotene, vitamin A, folic acid, potassium iodide, chromium chloride, sodium selenite, sodium molybdate, vitamin K_1, biotin, vitamin D_3, vitamin $B_{12.}$

The particle size distribution for the two puddings and the BSS was measured. The Figure 4.1 shows the results.

4.1.3 Milk

Whole milk powder from Alpura, which ingredients are: carbohydrates, dietary fiber, protein, lipids, potassium, calcium, phosphorus, magnesium, sodium, zinc, pantothenic acid, vitamins B_2, A, D and B_{12}.

4.1.4 Thickeners

The thickeners chosen for this research are commonly used in the diet for dysphagic patients. They are citrus pectin (Droguería Cosmopolita) and xanthan gum (Alfadelta). Below both are described.

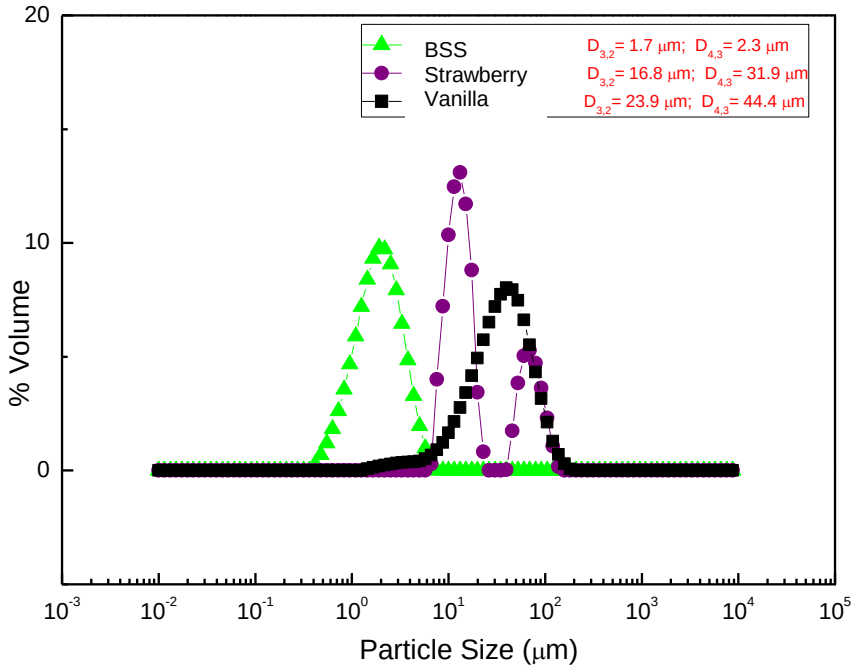

Figure 4.1. Particle size distribution for the BSS, vanilla pudding and strawberry pudding.

- Citrus Pectin

Citrus pectin is an abundant, ubiquitous and multifunctional component of the cell walls of all land plants. Their composition varies with plants, the conditions of extraction and other environmental factors. Citrus fruits are one of the most important sources of commercial citrus pectin (Willats, Knox, & Mikkelsen, 2006).

Citrus pectins are a group of oligosaccharides and polysaccharides that are extremely diverse in their fine structures (Ridley et al., 2001). They have in common the galacturonic acid (GalA), which comprises approximately 70% of citrus pectin. All the pectic polysaccharides contain GalA linked at the *O*-1 and the *O*-4 position (Mohnen, 2008).

- Xanthan gum

Xanthan gum is a polysaccharide produced by the bacterium *Xanthomonas campestris*. It is part of a group of materials that have an affinity for water and exhibit binding properties with water and other organic/inorganic materials (Palaniraj & Jayaraman, 2011).

It has a primary structure consisting of repeated pentasaccharide units formed by two glucose units, two mannose units, and one glucuronic acid unit. Its main chain consists of β-D-glucose units linked at the 1 and 4 positions. The backbone has attached a trisaccharide side chain, which contain a D-glucuronic acid unit between two D-mannose units linked at the O-3 position of every other glucose residue in the main chain.

4.1.5 Rheometers

- ARES (Rheometric Scientific, USA)

It is a strain-controlled rheometer equipped with a serrated plate and plate geometry (diameter 25 mm, gap 1 mm). This equipment has a range of rotational speeds from 0.00125 to 100 rad/s, with a minimum displacement angle that can be measured with a resolution of 0.01 rad. It has a forced convection oven with direct injection of air into the measuring chamber.

- MARS-HAAKE (Thermo-Haake, Germany)

It is a stress-controlled rheometer equipped with a serrated plate and plate geometry (35 mm diameter, 1 mm gap). Its torque range is 0.05 μNm to 200 mN m and the speed is 0.025 to 1200 rpm. The frequency range is 10^{-5} to 100 Hz with an angular resolution of 0.012 μrad. The rheometer incorporates a thermostatic bath (Phoenix, Thermo-Haake, Germany).

- Anton Paar (Physica MCR101, Austria)

It is a stress-controlled rheometer equipped with a plate and plate geometry (50 mm diameter, 1 mm gap). Its torque range is 0.1 μNm to 150 mN m. The speed ranges from 10^{-5} to 3000 1/min in controlled-rate mode and 10^{-6} to 3000 1/min in controlled-stress mode. The frequency ranges from 10^{-5} to 628 rad/s with an angular resolution of 0.01 μrad.

- Orifice rheometer

The extensional properties were measured in a orifice rheometer designed at the CCADET (Muñoz-Díaz, 2012; Naranjo, 2010). It consists of a profiled orifice located between two identical cylindrical reservoirs (Figure 4.2). The orifice is a cylinder with a profiled contraction having a ratio of 8:1:8 (Appendix A shows a detailed analysis of the profile orifice). Each reservoir has a capacity of 0.34 L and contains a piston, which pumps the working fluid from one reservoir to the other and then in the opposite direction. The cylindrical reservoirs have an inside diameter of 38.1 mm and they are long enough to generate fully developed flow upstream the orifice. The pressure is locally measured by means of pressure sensors having a range of 0 – 1380 kPa (0 – 200 psi) and an accuracy of 0.25% of full scale. They are placed upstream, downstream and in the contraction via small orifices. The volumetric flow rate is determined by the speed of the pistons. The pressure drop and the volumetric flow are used for calculating the extensional viscosity.

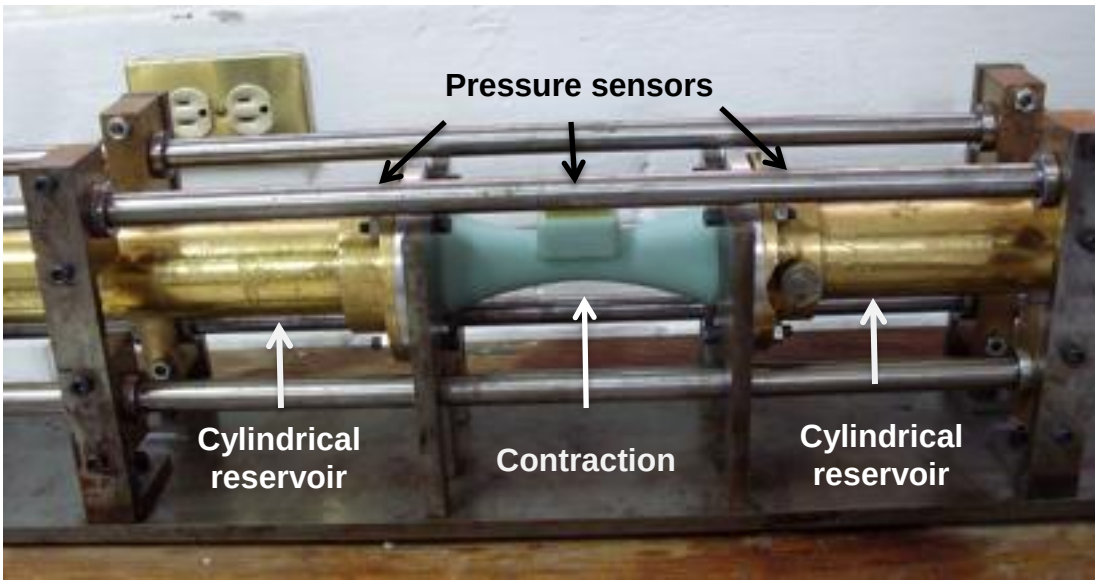

Figure 4.2. Orifice rheometer.

4.2 Methods

4.2.1 Thickened milk preparation

All the thickened milk samples were prepared with the same relationship water/milk (100 g/14 g), which is based on the manufacturer's recommendations. The samples prepared and their components are listed in Table 4.1.

Each ingredient was weighed in an analytical balance. Milk was mixed with the thickener and then water was added. This mixture was stirred for at least 30 minutes, until lumps disappeared. The samples were stored in refrigeration for 48 hours before being used. All the tests were run within five days of sample preparation in order to avoid decomposition.

4.2.2 Rheological measurements

The thickened milk samples were tested with the Anton Paar rheometer, which belongs to CCADET.

Table 4.1. Thickened milk sample prepared.

Sample	Xanthan gum % (w/w)	Citrus pectin % (w/w)	Milk % (w/w)	Water % (w/w)
X 2.6%	2.6	-	12.0	85.4
X 3.4%	3.4	-	11.9	84.7
X 3.6%	3.6	-	11.8	84.6
X 4.0%	4.0	-	11.8	84.2
X 4.4%	4.4	-	11.7	83.9
P 5.0%	-	5.0	11.7	83.3
P 6.6%	-	6.6	11.5	81.9
P 7.5%	-	7.5	11.4	81.1
P 8.0%	-	8.0	11.3	80.7

The puddings and the BSS were analyzed with two rheometers (ARES and MARS-HAAKE) from Universidad de Huelva. Extensional viscosity was measured with the same equipment in all cases. Table 4.2 gives more details about the samples and the equipment used.

The procedure to load a sample on the shear rheometers is described below:

- Anton Paar. Each sample was loaded in the rheometer's lower plate with special care. When the upper plate was lowered to the trim position the extra sample around the edge of the plate was trimmed with a metal spatula, and then the upper plate was lowered to the measurement position. Around the lower plate was added water and a container was placed over the upper plate, so a saturated environment was created to prevent evaporation in the sample. Then the sample was allowed to rest for 10 minutes before the test.

- ARES and MARS-HAAKE. Each sample was loaded with special care onto the rheometer. The sample filled up the entire gap. And after lowering upper plate the exposed edges of the sample were covered with liquid vaseline to prevent evaporation. The sample was allowed to rest for 10 minutes before the test.

Table 4.2. List of the rheometers used for each sample and test.

Test	Thickened milk	BSS	Puddings
Steady state viscous flow	Anton Paar	ARES	ARES
Steady state extensional flow	Orifice R.	Orifice R.	Orifice R.
Frequency sweep test	Anton Paar	MARS-HAAKE	MARS-HAAKE
Stress relaxation test	Anton Paar	ARES	ARES

4.2.4 Steady-state viscous flow

The puddings and BSS were analyzed in a shear rate range between 10^{-2} to 100 s^{-1}. A waiting time of 2 minutes between each point was used (Quinchia et al., 2011).Measurements were done in triplicate for each sample at 25 ºC.

In the thickened mill solutions was performed a test to determine the measuring point duration. The strain rate was set at 0.01 s^{-1} and the viscosity behavior was observed for 10 minutes. This procedure was repeated at 0.1, 1.0 and 100 s^{-1}. It was found that 2 minutes were sufficient for the sample to reach steady state. Although for speeds below 0.1 s^{-1} the time required was over 10 minutes, so it was decided to omit this range.

The test was performed with a $\dot{\gamma}$ logarithmic ramp from 0.1 to 100 s^{-1} and a measuring point duration profile of 2 minutes. Measurements were done in triplicate for each sample at 25 ºC.

The curve flow data of thickened milk solutions were compared with that of the BSS. The concentrations that matched the data of the BSS were selected to undergo the following tests.

4.2.5 Frequency sweep test

A stress sweep test at 1 Hz was done to determine the linear viscoelasticity region of the sample. The samples were analyzed in a stress range between 0.1-100 Pa.

A stress value, within the linear region, was chosen to perform a small amplitude oscillatory shear test. The samples were analyzed in a frequency range between 0.03 and 100 rad/s. A waiting time of 60 s between each point was used. Measurements were done in triplicate for each sample at 25 ºC.

4.2.6 Stress relaxation test

Stress relaxation curves, in the linear and non-linear viscoelasticity region, were obtained by applying different constant strains, comprised between 0.5 and 500%. Measurements were done in triplicate for each sample at 25 ºC.

4.2.7 Steady-state extensional flow

Each sample was loaded into one of the rheometer's reservoir. The sample was allowed to rest for 10 minutes. The test was performed with 8 measuring points in an extension rate between 100 – 1000 s^{-1} at room temperature (25 ºC).

4.3 Software and calculations

4.3.1 Data analysis

The software Microsoft was used to get the average of the triplicate measurements.

Origin 8.0 provides an extensive set of data analysis tools. This software was used to fit data from the steady-state viscous flow and extensional flow. For the first case it was used Sisko model due to it works well for dysphagia products (Quinchia et al., 2011). Power-law model was used to fit the data from the extensional measurements. The models and data were entered the software and then the curve fitting analysis was done.

4.3.2 Determination of the damping function values

The damping function values were calculated using the software Origin. Here we describe the stages of the procedure:

1. Chose a stress relaxation curve, within the linear range, as reference.
2. Draw the remaining stress relaxation curves (non-linear range) versus time in logarithmic scale.
3. Perform a vertical shift of the curves until they match the reference curve. Record the displacement factor ($h(\gamma)$) of each curve.

After applying the above procedure we get a pair of data; one corresponding to the applied strain, and the other one to the function damping. The Figure 4.4 shows an example.

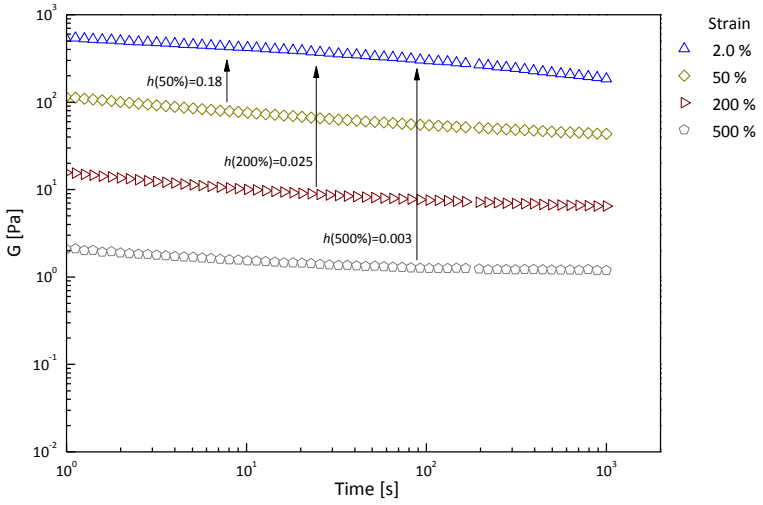

Figure 4.3. Determination of the damping function.

5 Results

In this section, the results for the shear viscosity, extensional viscosity, elastic modulus, viscous modulus and stress relaxation modulus will be described.

5.1 Steady-shear viscosity

Xanthan gum and citrus pectin were separately used to thick at different concentrations milk solutions, and then their steady-shear viscosity was measured. As can be seen in the Figure 5.1 all the samples show a shear thinning behavior, and their viscosity increases with increasing concentration. The flow curve data were fitted with Sisko model with a R^2 value greater than 0.999, the setting parameters are listed in the Table 5.1. The value for the flow index behavior (n) is in the range from 0.26 to 0.37 for the xanthan gum and 0.32 to 0.37 for the citrus pectin. Finally the values for the high shear rate limiting viscosity (η_∞) are in a range from 0.2 to 1.2 Pa s and 2.0 to 4.0 Pa s for the xanthan gum and citrus pectin respectively.

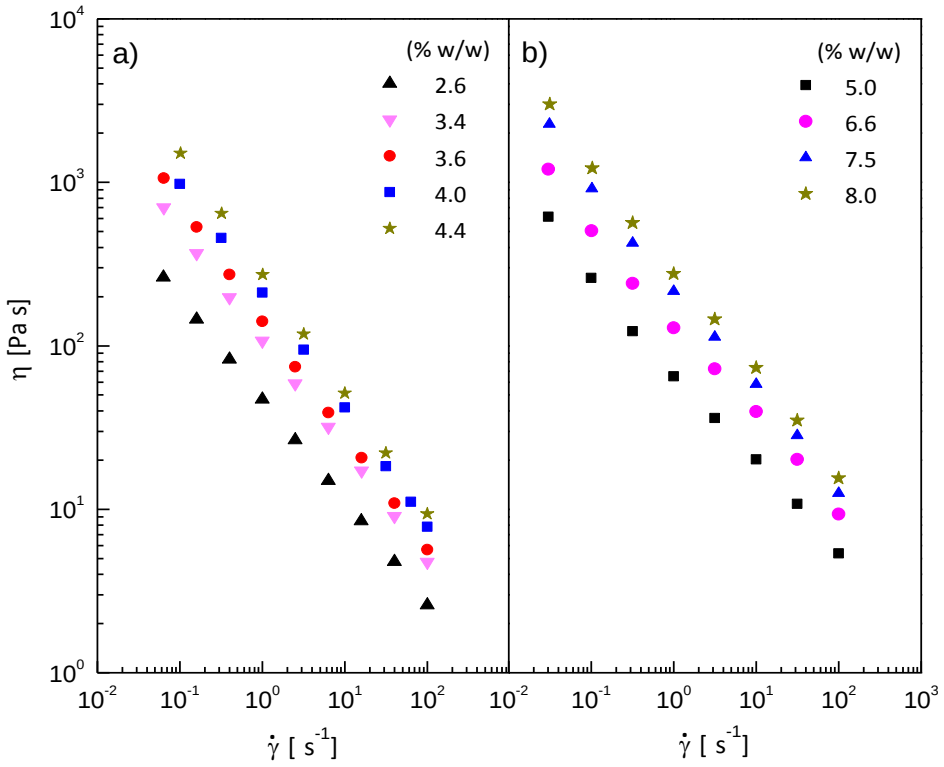

Figure 5.1. Steady-shear viscosity for the milk thickened samples as function of shear rate for: (a) xanthan gum and (b) citrus pectin.

In this work a commercial barium sulfate suspension (BSS) was used, which is a contrast fluid with spoon-thick consistency. The corresponding flow curve data are shown in the Figure 5.2. As may be seen the BSS shows a shear thinning behavior, with a value for n= 0.12.

The flow curve data from the thickened milk solutions were compared with those of the BSS, and the samples that matched their viscosity with that of the BSS were selected. The Figure 5.2 shows the flow curve data for the BSS compared with these samples: X 3.6%, X 4.4%, P 5.0% and P 8.0%.

Two kinds of pre-packed thickened food were selected for being analyzed in this work; they are labeled as vanilla pudding and strawberry pudding.

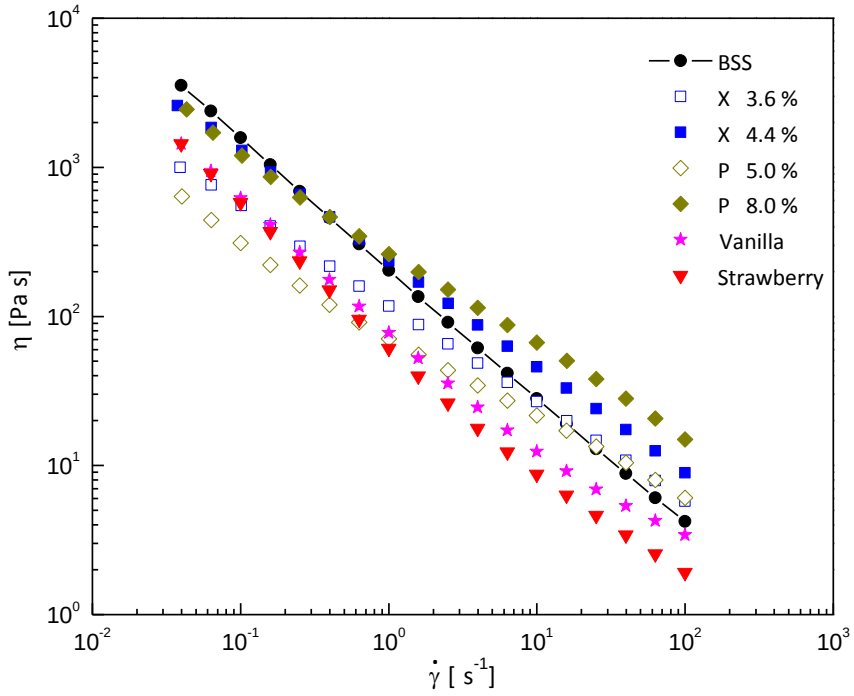

Figure 5.2. Steady-shear viscosity as function of shear rate for the BSS, puddings and thickened milk solutions.

The flow curve data from both are shown in the Figure 5.2. They have a shear thinning behavior with a value for n of 0.10 for the vanilla pudding and 0.05 for the strawberry pudding.

Looking at the Table 5.1 it is clear that the puddings have the lowest values for n, this mean that their viscosity decays quicker. They also show the lowest viscosity values at high strain as can be seen in the Figure 5.2. On the other hand the viscosity of the selected thickened milk solutions matches the viscosity of the BSS in different ranges; the higher concentrations do it at low shear rates, while the lower ones do it at high shear rates.

Table 5.1 Sisko model parameters for the BSS, thickened milk solutions and puddings.

Sample	K_2 (Pa s^n)	n (-)	η_∞ (Pa s)	R^2
BSS	206	0.12	0.7	0.9998
X 2.6%	46	0.37	0.3	0.9999
X 3.4%	104	0.31	0.8	0.9999
X 3.6%	138	0.26	1.2	0.9999
X 4.0%	210	0.28	0.3	0.9994
X 4.4%	277	0.26	0.2	0.9999
P 5.0%	66	0.37	2.0	0.9968
P 6.6%	130	0.37	2.7	0.9968
P 7.5%	220	0.33	3.0	0.9966
P 8.0%	280	0.32	4.0	0.9980
Vanilla	80	0.10	2.1	0.9975
Strawberry	65	0.05	1.1	0.9943

According to (Chen & Lolivret, 2011), the shear viscosity at 10 s^{-1} is a good parameter for being correlated with the sensory difficulty of swallowing. So this shear rate has been chosen to compare the BSS with the food for dysphagic patients studied in this work. Figure 5.3 shows the shear viscosity at 10 s^{-1} as a function of the thickeners concentration. The BSS, strawberry and vanilla sample has been included for purpose of comparison. It can be seen that xanthan gum has a higher thickening effect compared to citrus pectin. Also it is clear that the viscosity of the puddings is lower than the BSS, on the other hand the viscosity of milk thickened with xanthan gum (3.6%) matches the viscosity required at this shear rate.

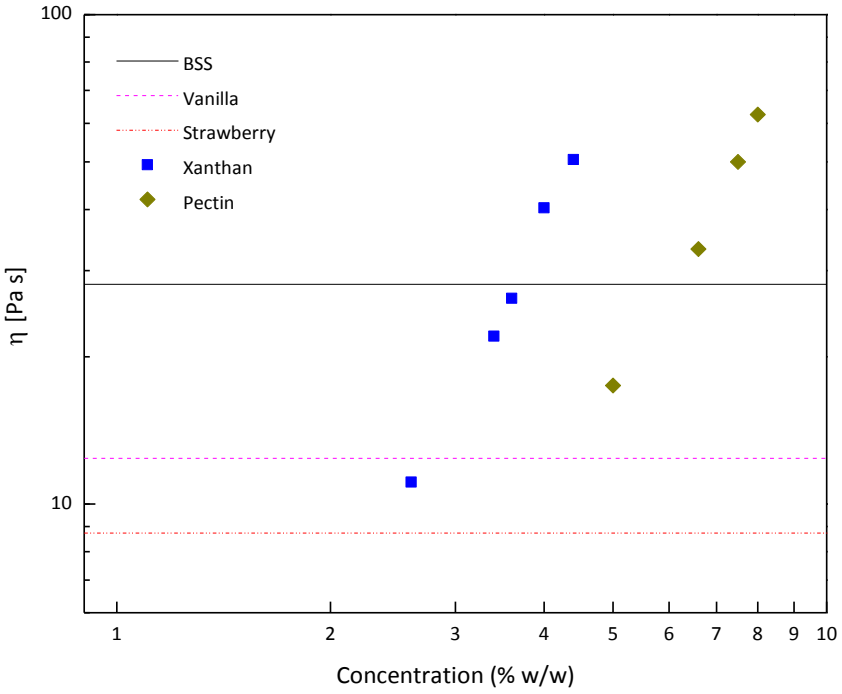

Figure 5.3. Steady-shear viscosity, at 10 s^{-1}, as a function of the thickener concentration.

5.2 Steady extensional viscosity

The extensional viscosity was measured in the BSS, puddings and thickened milk solutions. The Figure 5.4 shows the extensional viscosity as a function of the extension rate. It can be seen the samples show a decrease in the viscosity with increasing the extension rate.

Increasing the concentration of the citrus pectin increases the viscosity; however this not happens with the xanthan gum. The puddings show a similar viscosity between each other. At low extension rates the strawberry pudding and X 5.4% match the viscosity of the BSS, while in the remaining range X 3.6% matches the viscosity better.

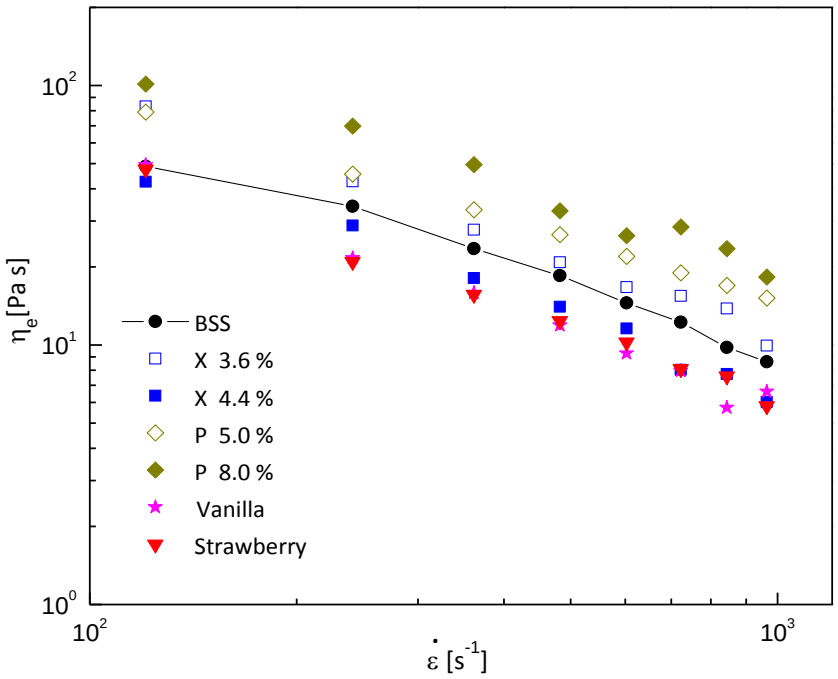

Figure 5.4. Steady-extensional viscosity as function of extension rate for the BSS, puddings and thickened milk solutions.

Table 5.2. Extensional power-law parameter.

Fluid	***l* (Pa s^t)**	***t* (-)**	**R^2**
BSS	2075	0.22	0.9902
X 3.6%	9081	0.02	0.9958
X 4.4%	5396	0.03	0.9649
P 5.0%	3557	0.21	0.9999
P 8.0%	6962	0.14	0.9641
Vanilla	4533	0.04	0.9750
Strawberry	5438	0.01	0.9986

The power-law model ($\eta_e = l\dot{\epsilon}^{t-1}$) was used to fit the data. The parameter t for the samples is in a range from 0.01 to 0.22, corresponding to the BSS the highest value and strawberry pudding the lowest. The P 5.0% sample has a value of t similar to that of the BSS. Most of the data fitted fairly well with the power-law model.

The Trouton ratio was calculated for comparing the extensional viscosity to the shear viscosity. The Figure 5.5 shows the Trouton ratio of the samples as a function of the effective strain rate. For comparison purposes, the Trouton ratio of 3 has been included in the plot.

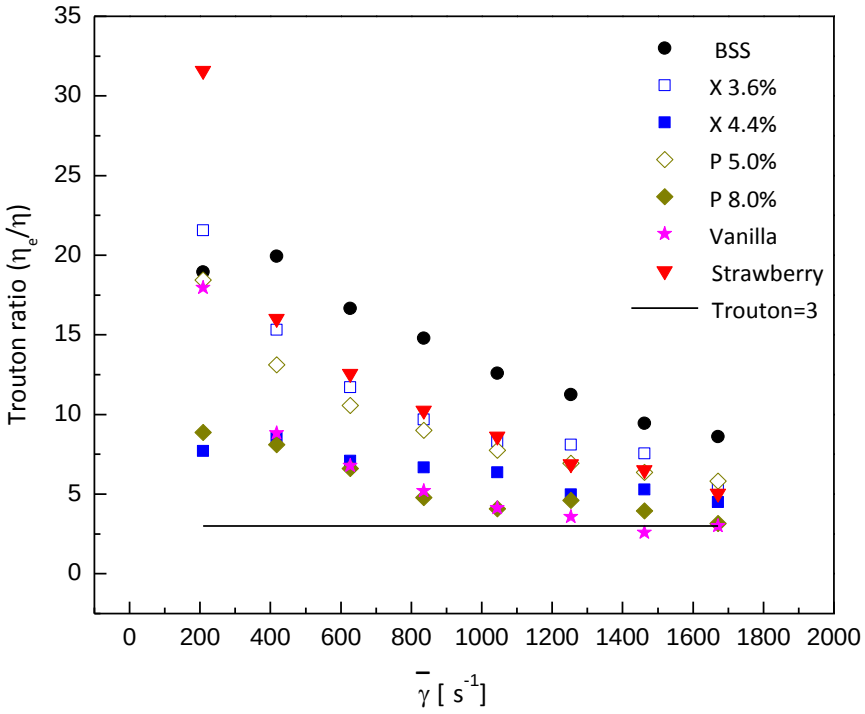

Figure 5.5. Trouton ratio as function of the effective strain rate for the BSS, puddings and thickened milk solutions.

The Trouton ratio of the thickened milk solutions (with low concentrations of thickener), puddings and BSS exceed by far the value expected for a Newtonian

fluid in the low effective strain region. When the effective strain rate increases the Trouton ratio decreases in all the samples. It is remarkable that the thickened milk solutions with the highest concentrations hardly change their ratio in the whole range studied. The BSS has the highest value in almost the entire range. The vanilla pudding and P 8.0% tend to a Newtonian behaviour before the other samples.

5.3 Elastic and viscous moduli

The Figure 5.6 shows the elastic (G') and viscous (G'') moduli as a function of the frequency for the thickened milk solutions. It can be seen that G' and G'' have a strong dependence on frequency, so they behave as a true polymer solution. Also it can be noticed that increasing the concentration of the thickener causes an increase of both moduli.

The Figure 5.7 shows G' and G'' as a function of the frequency for the puddings compared with the BSS. As can be seen the values of both moduli, of the two puddings, are higher than those of the BSS in the entire range of frequency. But in the tree samples G' is much larger than G'' in the whole range, so a solid-like behavior dominates. Also, both moduli have a slightly dependence on frequency, hence the two puddings and the BSS have a weak-gel like behavior.

The Figure 5.8 shows the radio G''/G' for all the samples. The BBS and the puddings show the lowest values, indicating that their elastic component is dominant; this behavior hardly changes in the frequency range studied. On the other hand in the thickened milk solutions G''/G' is closer to 1, which means that the viscous component is almost equal to the elastic component. In the case of the solutions with xanthan gum increasing the frequency causes an increase in the elastic component. The solution with citrus pectin at low concentration clearly shows an increase of the viscous component with increasing the frequency.

Moreover in both cases, xanthan gum and citrus pectin, it can be seen that increasing the concentration of the thickener favors an increase in the elastic characteristics.

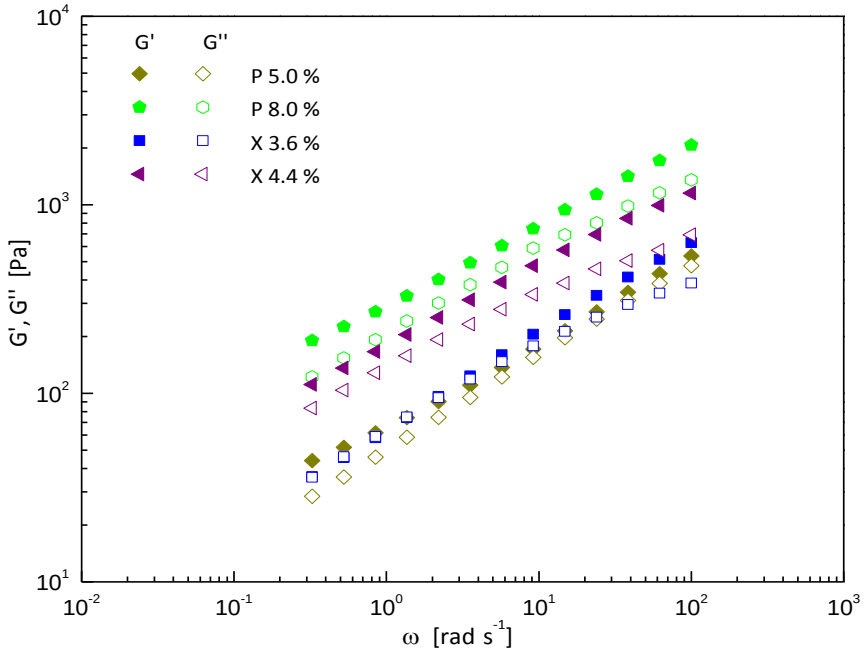

Figure 5.6. Evolution of the elastic and viscous moduli with frequency for X 3.6%, X 4.4%, P 5.0% and P 8.0%.

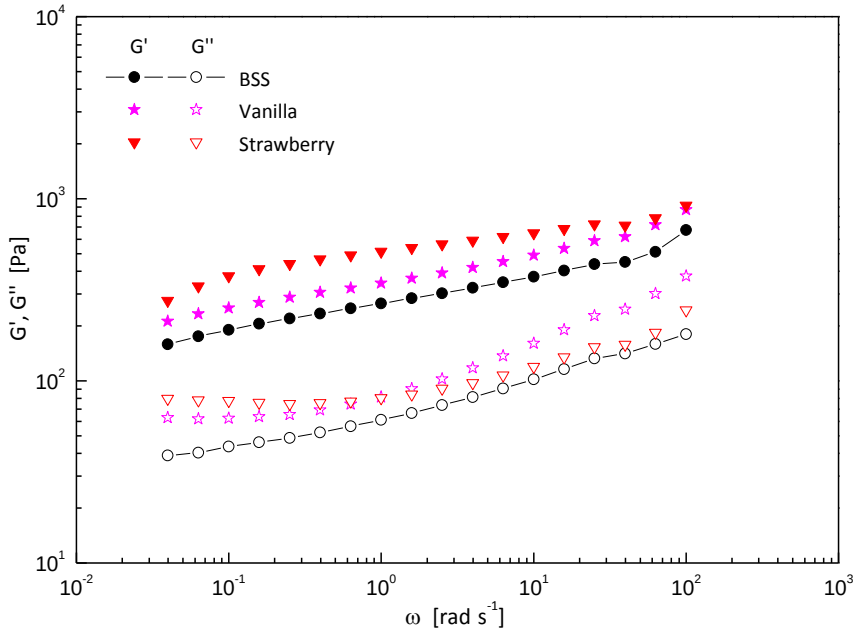

Figure 5.7. Evolution of the elastic and viscous moduli with frequency for the two puddings compared with BSS

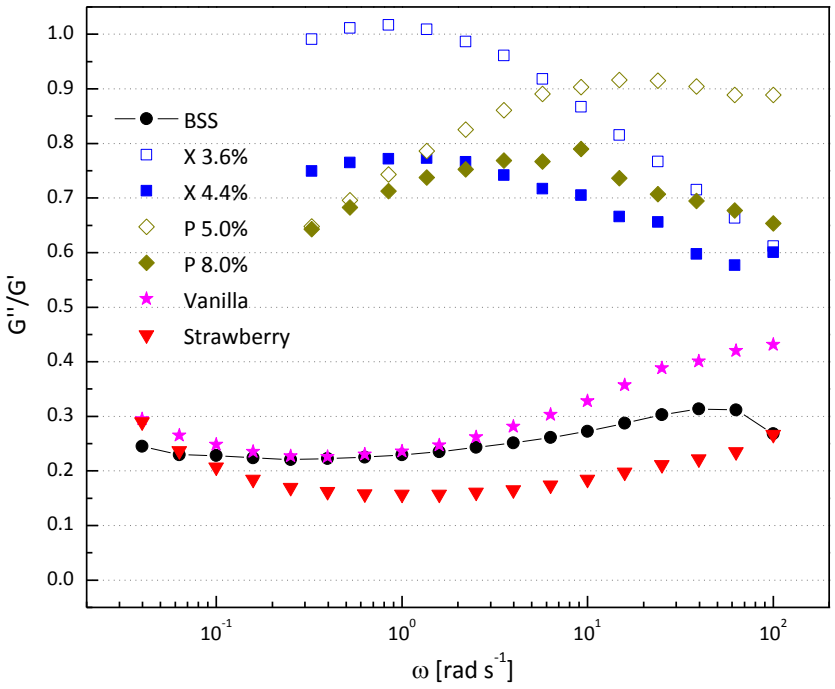

Figure 5.8. Evolution of G''/G' as function of frequency for the BSS, puddings and thickened milk solutions.

5.4 Complex viscosity

The Figure 5.9 shows the steady-shear viscosity (η) and complex viscosity (η*) as a function of shear rate and frequency for the BSS, puddings, and thickened milk solutions. In all the samples η* shows a shear thinning tendency. The BSS and milk thickened solutions whit xanthan gum show small differences between η and η*, while the milk thickened with citrus pectin and the puddings show larger differences. It can be seen that in the puddings η* is almost a decade higher than η.

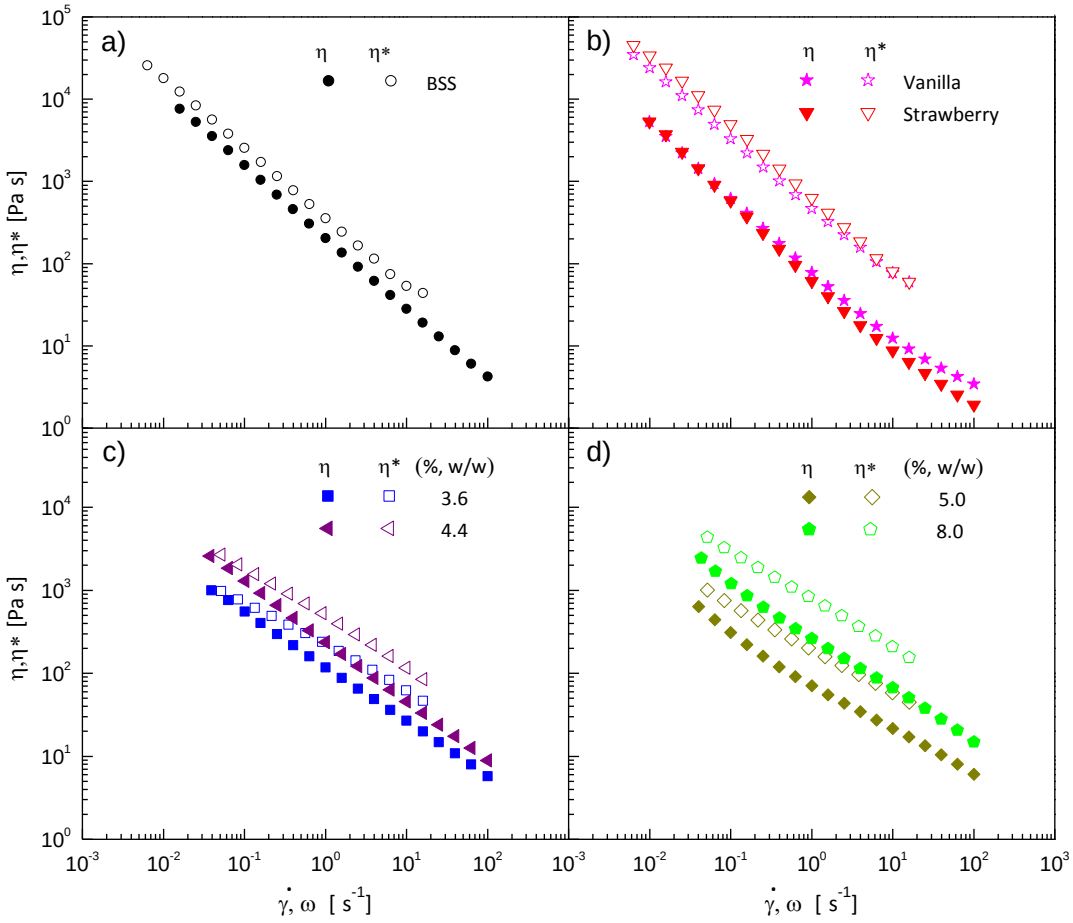

Figure 5.9. Steady-shear viscosity and complex viscosity as a function of shear rate and frequency for: (a) BSS, (b) puddings, (c) milk thickened whit xanthan gum and (d) milk thickened with citrus pectin.

5.5 Stress relaxation modulus

The Figure 5.10 shows the stress relaxation modulus $G(t)$ at different strains for the BSS, thickened milk solutions and puddings. It is clear that in all the cases $G(t)$ decreases with increasing time and strain. In the thickened milk solutions increasing the concentration of the thickener causes an increase of $G(t)$. In the puddings $G(t)$ is higher in the strawberry pudding.

From the stress relaxation modulus data was calculated the damping function (h), The Figure 5.11 shows h as a function of the strain for all the samples. In all the cases h decreases with increasing the strain. It can be seen that the X 4.4% has the highest values for h, while the strawberry has the lowest ones. The values of h for strawberry and vanilla puddings decrease quickly at low strains, and reach a plateau in 200%. In the thickened milk solutions the increase on the concentration of the thickener affects the values of h at the low strain range.

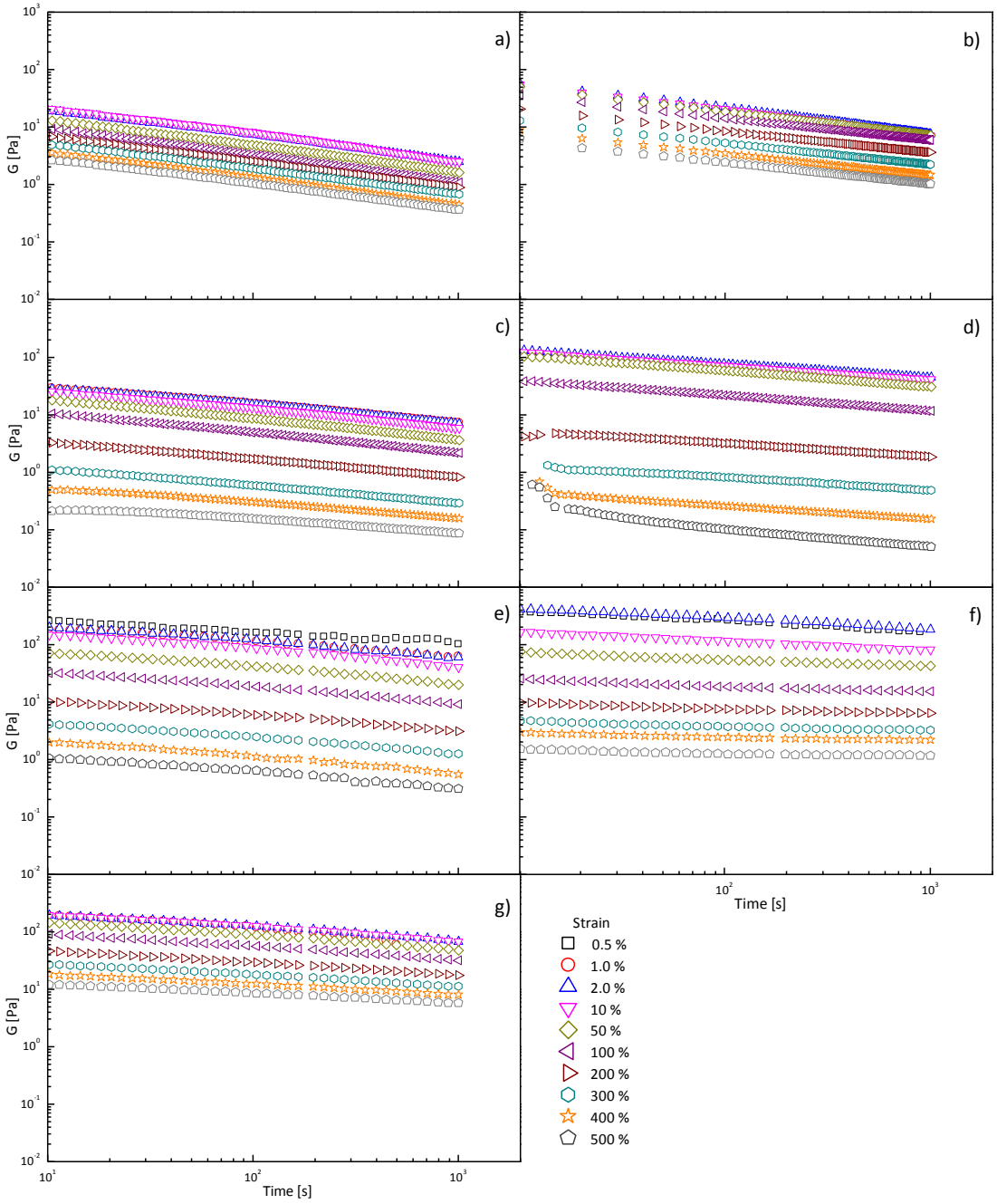

Figure 5.10. Relaxation modulus at different imposed constant strain conditions for: (a) X 3.6%, (b) X 4.4%, (c) P 5.0%, (d) P 8.0%, (e) vanilla pudding, (f) strawberry pudding and (g) BSS.

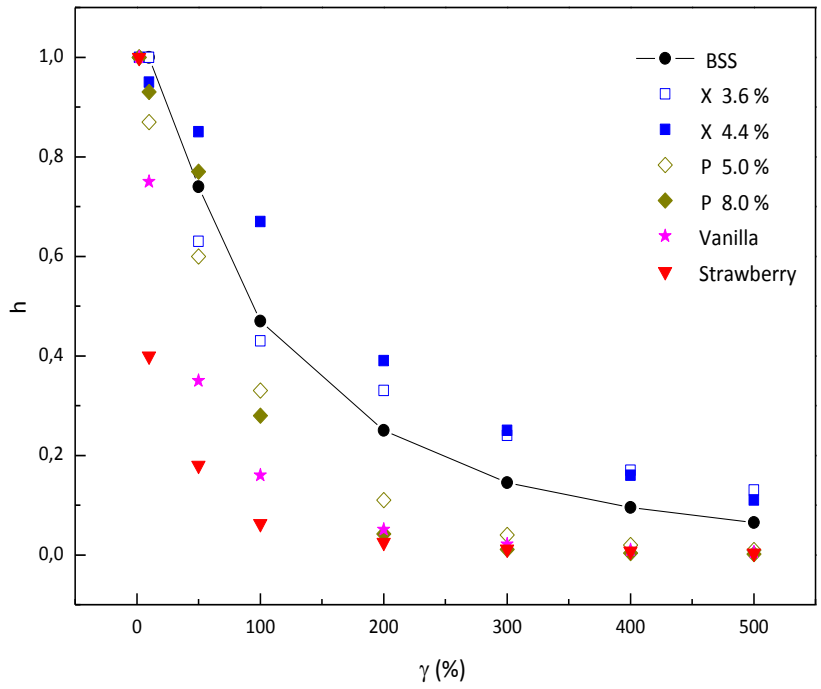

Figure 5.11. Evolution of the damping function for: BSS, X 3.6%, X 4.4%, P 5.0%, P 8.0%, vanilla and strawberry puddings.

6
Discussion

Throughout the present work we have determined the rheological behavior of a videofluoroscopic contrast fluid (BSS), two pre-packed thickened food for dysphagia, and milk solutions thickened separately with two kinds of thickeners. In this section the results described in the above section will be discussed.

It was found that all the samples have a shear thinning behavior, which is due to the alignment of the particles or macromolecules in the flow direction. All the samples showed an extensional thinning behavior over the whole extension rate range studied. However it was observed that some samples, that matched the shear viscosity of the BSS, do not do it with their extensional viscosity; like the milk thickened with citrus pectin. The samples thickened with xanthan gum showed a similar behavior to that observed in shear flow: the higher concentration matches the viscosity of the BSS at low strain rate, and the lower one do it at high extension rate. On the other hand the strawberry and vanilla sample showed again a lower viscosity than that of the BSS.

Also was found that an increase of the concentration of citrus pectin causes an increase in the extensional viscosity, but more interesting is that this not happen with the xanthan gum; for the thickener concentrations used there is an inverse relationship between the extensional viscosity and xanthan gum concentration.

Because of the orifice-rheometer limitations it was not possible to observe the behavior of the extensional viscosity at lower extension rates. However, for the range studied all the samples showed a thinning behavior. This may be explained by the decrease of the contacts/entanglements in the fluids with increasing the extension rate.

The Trouton ratio is useful to compare the extensional viscosity to the shear viscosity. As expected, the samples showed different responses to the extension strain and shear strain. Especially at low strains the samples showed an extensional viscosity higher than the shear viscosity.

A Trouton ratio of 3 is characteristic of a pure viscous fluid, when the ratio is higher the fluid have high elastic contributions (O'Brien & Mackay, 2002). It was seen that increasing the concentration of any of the thickeners decreases the Trouton ratio, so the samples show lower elastic contributions. The BSS showed the higher ratio in the whole range, so it has high elastic contributions.

The frequency sweep test showed that the thickened milk solutions behave as a true polymer solution, this means that the polymers form an entangled, so when the concentration increases there are more polymers increasing the entanglement, that's why G' increases too.

In the oscillatory tests high frequencies correspond to short times, and low frequencies relate to long times (Barnes, 2000). The thickened milk solutions, with the lowest concentrations, showed significant changes in G''/G'; the milk solution with xanthan gum, at long times, showed an elastic component almost equal to the viscous component. However, at short times its behavior is dominated by an elastic response. On the other hand in the milk solution with citrus pectin the behavior, at long times, is dominated by an elastic response, but at short times the viscous response becomes important.

Also it was observed that the steady-shear curves and dynamic data do not overlay, so the Cox-Merz rule does not apply. Most departures from the Cox–Merz rule are attributed to structure decay due to the effect of the strain

deformation applied to the system, which is low in oscillatory shear, but is high enough in steady-shear to break down structured intermolecular associations. Therefore, the complex viscosity is typically higher than the apparent shear viscosity in these cases. Thus departure from Cox-Merz rule may imply strong inter and intramolecular associations (Lopes da Silva et al., 1993). Because of this it seems that the BSS have the strongest associations, and the puddings have the weakest. This may explain why the puddings show a viscosity lower than the BSS, in shear and extensional flow.

Finally it was found that all the relaxation curves at different strains exhibited similar time dependence, and they appeared to be merely translations along the modulus axis. Therefore it was possible to propose that the relaxation modulus depends on two variables; one is a function of time ($G(t)$) and the other one is a function of the strain ($h(\gamma)$).

The damping function reflects the shear resistant of the sample under deformations outside the linear viscoelasticity range (Quinchia et al., 2011). It was found that the microstructure of the BSS and the milk thickened with xanthan gum was the most shear resistant while that of the puddings suffers a significant destruction. This is probably due to the BSS and the thickened milk solutions have stronger associations than the puddings, as mentioned above.

7
Conclusions

1. According to the study the milk solutions thickened with xanthan gum at 3.6% and 4.4% are the most suitable for patients who responded well to the contrast fluid with spoon-thick consistency. The extensional viscosity of two pre-packed thickened foods, two milk solutions thickened with xanthan gum, two milk solutions thickened with citrus pectin, and a contrast fluid with spoon-like consistency was evaluated. Although all the samples showed an extensional viscosity similar to that of the contrast fluid, the viscosity of the milk solutions with xanthan gum was the closest to the viscosity of the contrast fluid.
2. The shear viscosity of two pre-packed thickened foods and one contrast fluid with spoon-thick consistency was measured. In both cases it was observed a shear thinning behavior, although the viscosity of the contrast fluid was higher than that of the pre-packed foods in the shear rate range studied.
3. The shear viscosity of milk solutions thickened with xanthan gum at several concentrations (2.6, 3.4, 3.6, 4.0, 4.4 % w/w) and milk solutions thickened with citrus pectin (5.0, 6.6, 7.5, 8.0 % w/w) was measured. All the samples showed a shear thinning behavior and an increase in the viscosity with increasing the thickener concentration.
4. The shear viscosity of two milk solutions thickened with xanthan gum (3.6% and 4.4%) and two milk solutions thickened with citrus pectin (5.0% and

8.0%) matched the shear viscosity of the contrast fluid. These solutions were selected.

5. The extensional viscosity of the milk solutions selected, the pre-packed thickened foods and the contrast fluid was measured using an orifice rheometer designed in the CCADET. In the extension rate range studied (100-1000 s^{-1}) the milk solutions thickened with citrus pectin showed the highest viscosity, while the pre-packed foods showed the lowest. All the samples showed a thinning behavior.
6. The elastic and viscous moduli of the samples were measured in an oscillatory test. In the thickened milk solutions both moduli showed a strong dependence on frequency, on the other hand the moduli of the pre-packed foods and the contrast fluid showed a slightly dependence on frequency.

   The stress relaxation modulus of the samples was measured. In all the samples the modulus decreased with increasing time and strain.

8

Recommendations

- In this work it was measured the extensional viscosity only for two concentrations of each thickener but it should be tested more concentrations and other food thickeners since these information may contribute to broad diets of dysphagia patients.
- The orifice rheometer used in this work is able to work in a strain range from 100 to 1000 s^{-1}. It is recommended to modify the equipment in order to measure the viscosity at lower strains.

Appendix A

This section shows the analysis done for designing the profiled contraction used in the orifice rheometer. The reader is referred to Muñoz-Díaz (2012) for more information.

Consider the flow of a fluid in a pipe that has a contraction. The following assumptions are considered:

1. **Irrotational flow**
2. **Steady flow**
3. **Incompressible flow**
4. **Tubular flow**
5. $\boldsymbol{v_\theta = 0}$ (0)

The Figure A1 shows the flow pattern in cylindrical coordinates.

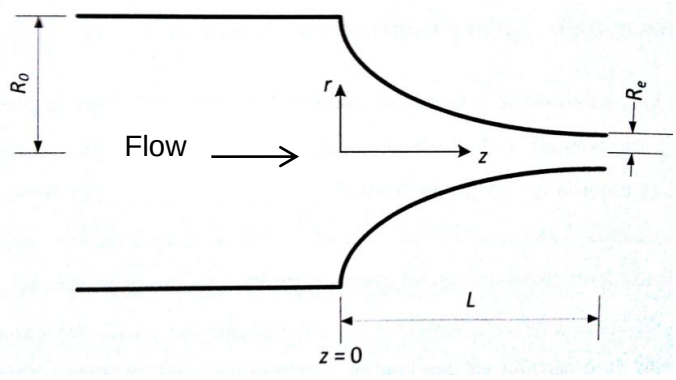

Figure A1. Flow in a pipe and its contraction.

The extensional rate is:

$$\dot{\epsilon} = \frac{\partial v_z}{\partial z} \tag{1}$$

Using a contraction with small dimensions allows assuming that $\dot{\epsilon}$ is constant. By separating variables, and then integrating each side of (1):

$$v_z = \dot{\epsilon} z + f(r) \tag{2}$$

Where $f\ (r)$ is the constant of integration.

On the other hand the continuity equation in cylindrical coordinates is:

$$\frac{1}{r}\frac{\partial (r v_r)}{\partial r} + \frac{1}{r}\frac{\partial v_\theta}{\partial \theta} + \frac{\partial v_z}{\partial z} = 0 \tag{3}$$

Since $v_\theta = 0$:

$$\frac{1}{r}\frac{\partial (r v_r)}{\partial r} + \frac{\partial v_z}{\partial z} = 0$$

Substituting the equation (1):

$$\frac{1}{r}\frac{\partial (r v_r)}{\partial r} + \dot{\epsilon} = 0$$

Separating variables and integrating:

$$r v_r = -\frac{1}{2} r^2 \dot{\epsilon} + g(z)$$

$$v_r = -\frac{1}{2} r \dot{\epsilon} + \frac{1}{r} g(z) \tag{4}$$

Where $g\ (z)$ is the constant of integration.

Because the flow is assumed irrotational:

$$\nabla \times \bar{u} = 0$$

Where $\bar{u}$ is the velocity vector. Developing:

$$\nabla \times \bar{u} = \begin{vmatrix} \hat{e}_r & \hat{e}_\theta & \hat{e}_z \\ \dfrac{\partial}{\partial r} & \dfrac{1}{r}\dfrac{\partial}{\partial \theta} & \dfrac{\partial}{\partial z} \\ v_r & r v_\theta & v_z \end{vmatrix}$$

$$\nabla \times \bar{u} = \left[\frac{1}{r}\frac{\partial v_z}{\partial \theta} - \frac{\partial (r v_\theta)}{\partial z}\right]\hat{e}_r + \left[\frac{\partial v_r}{\partial z} - \frac{\partial v_z}{\partial r}\right]\hat{e}_\theta + \left[\frac{\partial (r v_\theta)}{\partial r} - \frac{1}{r}\frac{\partial v_r}{\partial \theta}\right]\hat{e}_z = 0$$

Since $v_\theta = 0$:

$$\left[\frac{1}{r}\frac{\partial v_z}{\partial \theta}\right]\hat{e}_r + \left[\frac{\partial v_r}{\partial z} - \frac{\partial v_z}{\partial r}\right]\hat{e}_\theta - \left[\frac{1}{r}\frac{\partial v_r}{\partial \theta}\right]\hat{e}_z = 0$$

Then each component is matched to zero:

$$\frac{1}{r}\frac{\partial v_z}{\partial \theta} = 0 \tag{5}$$

$$\frac{\partial v_r}{\partial z} - \frac{\partial v_z}{\partial r} = 0 \tag{6}$$

$$-\frac{1}{r}\frac{\partial v_r}{\partial \theta} = 0 \tag{7}$$

Deriving (2) and (4) with respect to r and z, respectively:

$$\frac{\partial v_z}{\partial r} = \frac{\partial}{\partial r}[\dot{\epsilon} z + f(r)] = \frac{\partial f(r)}{\partial r} \tag{8}$$

$$\frac{\partial v_r}{\partial z} = \frac{\partial}{\partial z}\left[-\frac{1}{2} r \dot{\epsilon} + \frac{1}{r} g(z)\right] = \frac{1}{r}\frac{\partial g(z)}{\partial z} \tag{9}$$

Substituting (8) and (9) in (6):

$$\frac{1}{r}\frac{\partial g(z)}{\partial z} - \frac{\partial f(r)}{\partial r} = 0$$

$$\frac{\partial g(z)}{\partial z} = r\frac{\partial f(r)}{\partial r} \tag{10}$$

Then:

$$\frac{dg(z)}{dz} = C \tag{11}$$

$$r\frac{df(r)}{dr} = C \tag{12}$$

Where C is a constant. Resolving (11) and (12):

$$g(z) = Cz + A \tag{13}$$

$$f(r) = C\mathrm{In}r + B \tag{14}$$

Where A and B are the constants of integration. Substituting (14) in (2) and (13) in (4):

$$v_z = \dot{\epsilon}z + C\mathrm{In}r + B \tag{15}$$

$$v_r = -\frac{1}{2}r\dot{\epsilon} + \frac{1}{r}(Cz + A) \tag{16}$$

If $r \to 0$ also $v_r \to 0$, then C and A must be equal to zero.

$$v_z = \dot{\epsilon}z + B \tag{17}$$

$$v_r = -\frac{1}{2}r\dot{\epsilon} \tag{18}$$

Where B is a constant that represents the initial axial velocity. The rate of deformation tensor is:

$$\overline{\overline{\mathrm{D}}} = \nabla\bar{u} + (\nabla\bar{u})^T \tag{19}$$

where the velocity gradient tensor in cylindrical coordinates is:

$$(\nabla\bar{u})^T = \begin{vmatrix} \dfrac{\partial v_r}{\partial r} & \dfrac{\partial v_\theta}{\partial r} & \dfrac{\partial v_z}{\partial r} \\ \left(\dfrac{1}{r}\dfrac{\partial v_r}{\partial \theta} - \dfrac{v_\theta}{r}\right) & \left(\dfrac{1}{r}\dfrac{\partial v_\theta}{\partial \theta} + \dfrac{v_r}{r}\right) & \dfrac{1}{r}\dfrac{\partial v_z}{\partial \theta} \\ \dfrac{\partial v_z}{\partial z} & \dfrac{\partial v_\theta}{\partial z} & \dfrac{\partial v_z}{\partial z} \end{vmatrix}$$

Substituting $v_\theta = 0$, (17) and (18) in (19):

$$\overline{\overline{\mathrm{D}}} = \begin{vmatrix} -\dfrac{1}{2}\dot{\epsilon} & 0 & 0 \\ 0 & -\dfrac{1}{2}\dot{\epsilon} & 0 \\ 0 & 0 & \dot{\epsilon} \end{vmatrix} + \begin{vmatrix} -\dfrac{1}{2}\dot{\epsilon} & 0 & 0 \\ 0 & -\dfrac{1}{2}\dot{\epsilon} & 0 \\ 0 & 0 & \dot{\epsilon} \end{vmatrix}$$

$$\overline{\overline{\mathrm{D}}} = \begin{vmatrix} -\dot{\epsilon} & 0 & 0 \\ 0 & -\dot{\epsilon} & 0 \\ 0 & 0 & 2\dot{\epsilon} \end{vmatrix} \tag{20}$$

The equation (20) shows that for the velocities defined by the equations (0), (17) and (18) the flow is only extensional. Now it will be found the profile of the contraction that satisfies these same equations.

Assuming a steady flow the streamlines provide the shape of the contraction. For the two-dimensional field r-z:

$$\frac{dr}{v_r} = \frac{dz}{v_z} \tag{21}$$

Arranging (21) and substituting (17) and (18):

$$\frac{dr}{dz} = \frac{v_r}{v_z} = \frac{-\frac{1}{2}r\dot{\epsilon}}{\dot{\epsilon}z + B} = -\frac{r}{2(z + B/\dot{\epsilon})} \tag{22}$$

$B/\dot{\epsilon}$ is a constant, so:

$$N = \frac{B}{\dot{\epsilon}} \tag{23}$$

Substituting in (22) and separating variables:

$$\frac{dr}{r} = -\frac{dz}{2(z + N)}$$

Integrating:

$$\ln r = -\frac{1}{2}\ln (z + N) + \ln\left(M^{\frac{1}{2}}\right)$$

$$\ln r = -\ln (z + N)^{\frac{1}{2}} + \ln\left(M^{\frac{1}{2}}\right)$$

$$\ln r = \ln\left(\frac{M^{\frac{1}{2}}}{(z + N)^{\frac{1}{2}}}\right)$$

$$r^2 = \frac{M}{z + N} \tag{24}$$

The last equation is a semihyperbolyc profile which radio r is a function of the variable z. The constants M and N are obtained using the geometric values of the Figure A1: R_0 in $z = 0$ and R_e in $z = L$.

$$R(0) = R_0 \;\rightarrow\; R_0^2 = \frac{M}{N}$$

$$R(L) = R_e \;\rightarrow\; R_e^2 = \frac{M}{L + N}$$

Solving for M and N:

$$M = \frac{LR_0^2 R_e^2}{R_0^2 - R_e^2} \tag{25}$$

$$M = \frac{LR_0^2 R_e^2}{R_0^2 - R_e^2} \tag{26}$$

The equations (24), (25) and (26) are used for generating the semihyperbolyc profile used in the experimental work.

A steady, incompressible, irrotational flow through a semihyperbolic converging die defined by

$$r^2 = \frac{M}{z + N}$$

has a velocity field given by

$$v_z = \dot{\epsilon} z + B$$

$$v_r = -\frac{1}{2} r \dot{\epsilon}$$

$$v_\theta = 0$$

with a constant extensional rate $\dot{\epsilon}$.

Determination of extensional viscosity.

The extensional viscosity for the flow in the contraction is:

$$\eta_e = \frac{\sigma_{zz} - \sigma_{rr}}{\dot{\epsilon}} \tag{27}$$

In this case the strain rate $\dot{\epsilon}$ is constant, the problem now is to determine $\sigma_{zz} - \sigma_{rr}$.

Consider the energy equation:

$$\frac{DH}{Dt} = \nabla \cdot \bar{q} + \bar{\bar{\sigma}} : \nabla \bar{u} + \frac{DP}{Dt}$$

where

H = Total enthalpy

$\bar{q}$ = Heat transferred

$\bar{\bar{\sigma}}$ = Stress tensor

P = Static pressure

Other assumptions are the following:

1. **Isothermal flow**
2. **Shear-free flow**
3. **Negligible inertial terms**
4. **Whereas the diameter of the orifice is small, then $\boldsymbol{\sigma_{rr} = \sigma_{\theta\theta}}$**
5. **Because of the size of the contraction: $\boldsymbol{\frac{\partial P}{\partial r} = \frac{\partial P}{\partial \theta} = 0}$**

Then the energy equation is:

$$-\bar{u} \cdot \nabla \mathrm{P} = \bar{\bar{\sigma}} : \nabla \bar{u} \qquad (28)$$

Developing the left side of (28):

$$\bar{u} \cdot \nabla \mathrm{P} = (v_r \hat{e}_r + v_\theta \hat{e}_\theta + v_z \hat{e}_z) \cdot \left(\frac{\partial y}{\partial x} \hat{e}_r + \frac{1}{r} \frac{\partial P}{\partial \theta} \hat{e}_\theta + \frac{\partial P}{\partial z} \hat{e}_z \right) = v_z \frac{\partial P}{\partial z} \qquad (29)$$

Developing the right side of (28):

$$\bar{\bar{\sigma}}:\nabla\bar{u}=\begin{vmatrix}\sigma_{rr} & \sigma_{r\theta} & \sigma_{rz}\\ \sigma_{\theta r} & \sigma_{\theta\theta} & \sigma_{\theta z}\\ \sigma_{zr} & \sigma_{z\theta} & \sigma_{zz}\end{vmatrix}:\begin{vmatrix}-\frac{1}{2} & 0 & 0\\ 0 & -\frac{1}{2}\dot{\epsilon} & 0\\ 0 & 0 & \dot{\epsilon}\end{vmatrix}=-\frac{1}{2}\dot{\epsilon}\sigma_{rr}-\frac{1}{2}\dot{\epsilon}\sigma_{\theta\theta}+\dot{\epsilon}\sigma \tag{30}$$

The trace of the tensor must be equal to zero:

$$\sigma_{rr}+\sigma_{\theta\theta}+\sigma_{zz}=2\sigma_{rr}+\sigma_{zz}=0$$

$$\sigma_{rr}=-\frac{1}{2}\sigma_{zz} \tag{31}$$

Substituting in (31) in (30):

$$\bar{\bar{\sigma}}:\nabla\bar{u}=-\dot{\epsilon}\sigma_{rr}-\dot{\epsilon}\sigma_{zz}=-\dot{\epsilon}\left(-\frac{1}{2}\sigma_{zz}\right)+\dot{\epsilon}\sigma_{zz}=\frac{3}{2}\dot{\epsilon}\sigma_{zz} \tag{32}$$

Substituting (29) and (32) in (28):

$$-\nu_z\frac{\partial P}{\partial z}=\frac{3}{2}\dot{\epsilon}\sigma_{zz} \tag{33}$$

Substituting (17) in (33), separating variables and integrating:

$$-\Delta\mathrm{P}=\frac{3}{2}\dot{\epsilon}\int_{t_0}^{t_e}\left(\frac{\sigma_{zz}}{\dot{\epsilon}z+B}\right)dt \tag{34}$$

Given the equation:

$$\frac{dz}{dt}=v_z=\dot{\epsilon}z+B$$

So that:

$$dz=(\dot{\epsilon}z+B)dt$$

Substituting in (34):

$$-\Delta \mathrm{P} = \frac{3}{2}\dot{\epsilon}\int_{t_0}^{t_e}\sigma_{zz}dt \tag{35}$$

σ_{zz} is constant in the contraction, at least for a pseudoplastic fluid that is a non-Newtonian fluid, then:

$$-\Delta \mathrm{P} = \frac{3}{2}\dot{\epsilon}\sigma_{zz}(t_e - t_0) \tag{36}$$

The Hencky strain is defined as (Macosko, 1994):

$$\epsilon_h = \dot{\epsilon}(t_e - t_0) = \ln\left(\frac{A_0}{A_e}\right) = \ln\left(\frac{R_0^2}{R_e^2}\right) \tag{37}$$

Substituting in (36):

$$\sigma_{zz} = -\frac{2}{3}\frac{\Delta \mathrm{P}}{\epsilon_h} \tag{38}$$

Finally, substituting (31) and (38) in (27):

$$\eta_e = \frac{\sigma_{zz} + \frac{1}{2}\sigma_{rr}}{\dot{\epsilon}} = \frac{3\sigma_{zz}}{2\dot{\epsilon}} = -\frac{3}{2\dot{\epsilon}}\left(\frac{2}{3}\frac{\Delta \mathrm{P}}{\epsilon_h}\right)$$

$$\eta_e = -\frac{\Delta \mathrm{P}}{\dot{\epsilon}\epsilon_h} \tag{39}$$

Equation (39) suggests that the extensional viscosity can be determined by measuring the pressure drop and the extension rate through the contraction. This analysis is valid if the extension rate is constant.

The contraction designed from (24), (25), and (26) is symmetric in the flow direction, with a semihyperbolic profile. The Figure A2 shows the dimensions of the contraction.

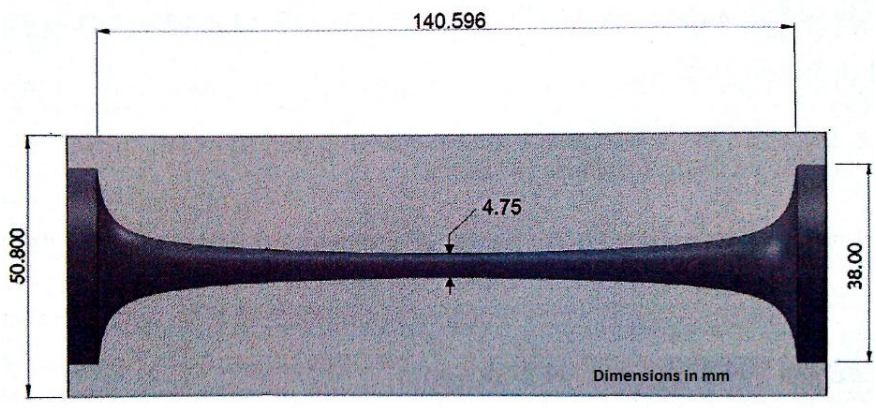

Figure A2. Semihyperbolic contraction designed (dimensions in mm).

Adapted from: Muñoz-Díaz (2012).

Experimentally $\dot{\epsilon}$ is calculated using the following expression which is valid for a semihyperbolic contraction (Feigl, Tanner, Edwards, & Collier, 2003):

$$\dot{\epsilon} = \frac{Q}{\pi R_0^2 L}(e^{\epsilon_h} - 1) \tag{40}$$

Where Q is the volumetric flow and L in length of the contraction. Using (37) the Hencky strain is:

$$\epsilon_h = \ln\left(\frac{R_0^2}{R_e^2}\right) = \ln\left(\frac{19.05^2}{2.375^2}\right) = 4.158$$

Simulations and experimental study

The validity of the assumptions considered was corroborated by means of 3D simulations, using the software Fluent©. In the computational model the wall

condition was considered as complete slip between fluid and wall. Further an experimental work was done using the semihyperbolic contraction.

Newtonian and non-Newtonian fluids were used in the experimental study and in the simulations. The Newtonian fluids were corn syrup (μ=0.56 Pa s and ρ=1038 kg/m^3) and an aqueous solution of polyethylene glycol at 60% in weight (μ=6.28 Pa s and ρ=1084 kg/m^3). The non-Newtonian fluid was an aqueous solution of polyethylene glycol (59% w/w) with carboxymethyl cellulose (1% w/w). The Figure A3 shows the Trouton ratio (ratio of extensional viscosity to shear viscosity) as a function of the strain rate for a Newtonian fluid (corn syrup).

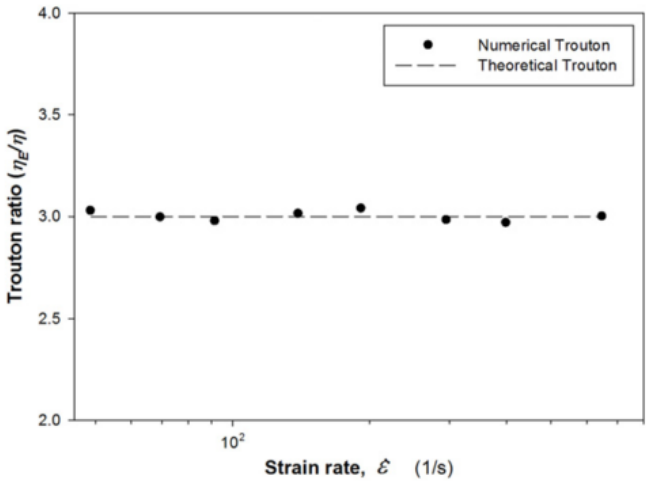

Figure A3. Trouton ratio as a function of the strain rate for a Newtonian fluid.

Adapted from: Muñoz-Díaz et al. (2012)

The Figure A4 shows the extensional viscosity from the simulation and the experimental study for the aqueous solution of polyethylene glycol (Newtonian fluid). And the Figure A5 shows the extensional viscosity from the simulation and the experimental study for the aqueous solution of polyethylene glycol with carboxymethyl cellulose (non-Newtonian fluid).

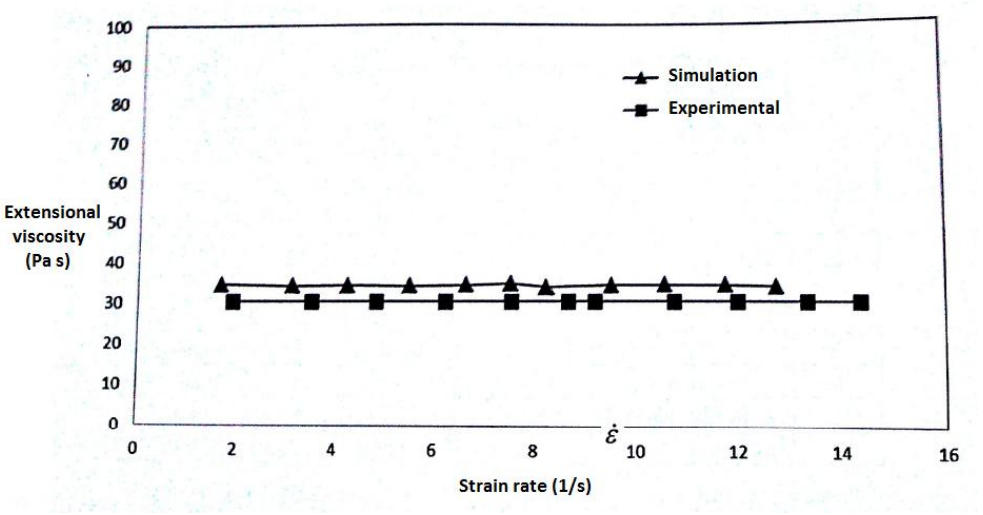

Figure A4. Extensional viscosity for the aqueous solution of polyethylene glycol.

Adapted from: Muñoz-Díaz (2012)

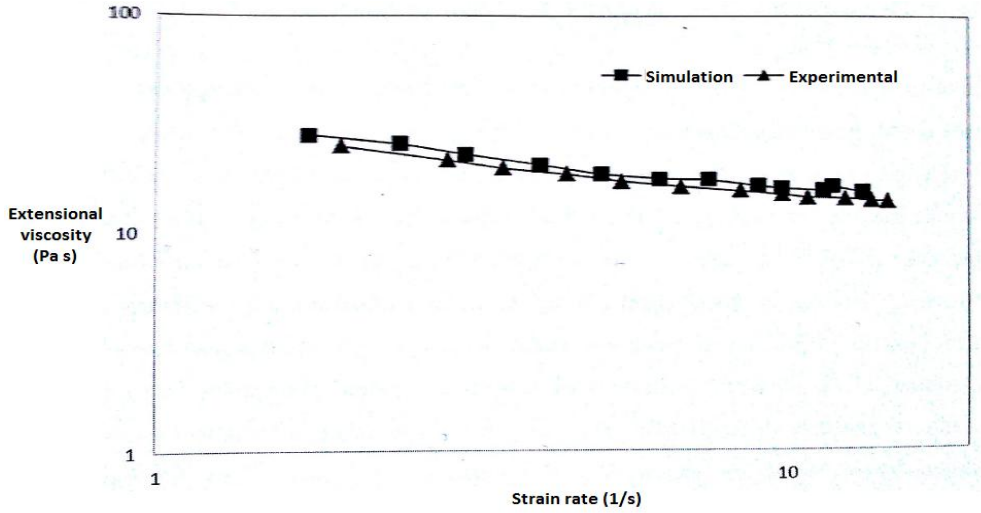

Figure A5. Extensional viscosity for the aqueous solution of polyethylene glycol with carboxymethyl cellulose.

Adapted from: Muñoz-Díaz (2012)

Literature cited

Ascanio, G., Carreau, P. J., Brito-de la Fuente, E., & Tanguy, P. A. (2002). Orifice flowmeter for measuring extensional rheological properties. *The Canadian Journal of Chemical Engineering*, *80*(December), 1189–1196.

Bardan, E., Kern, M., Arndorfer, R. C., Hofman, C., & Shaker, R. (2006). Effect of aging on bolus kinematics during the pharyngeal phase of swallowing. *American Journal of Physiology-Gastrointestinal and Liver Physiology*, *290*(3), G458–G465.

Barnes, H. A. (2000). *A handbook of elementary rheology*. Aberystwyth: University of Wales, Institute of Non-Newtonian Fluid Mechanics.

Barnes, H. A., Hutton, J. F., & Walters, K. (1989). *An introduction to rheology*. Amsterdam, Holland: Elsevier.

Brito-de la Fuente, E., Ekberg, O., & Gallegos, C. (2012). Rheological aspects of swallowing and dysphagia. *Dysphagia*, 493–506.

Brito-de la Fuente, E., Quinchia, L., & Valencia, C. (2010). Rheology of a new spoon-thick consistency oral nutricional supplement (ONS) in comparison with a swallow barium test feed (SBTF). *Dysphagia*, *25*(4), 362–362.

Buettner, A., Beer, A., Hannig, C., & Settles, M. (2001). Observation of the swallowing process by application of videofluoroscopy and real-time magnetic resonance imaging-consequences for retronasal aroma stimulation. *Chemical senses*, *26*(9), 1211–1219.

Casanovas, A., Hernández, M. J., Martí-Bonmatí, E., & Dolz, M. (2011). Cluster classification of dysphagia-oriented products considering flow, thixotropy and oscillatory testing. *Food Hydrocolloids*, *25*(5), 851–859.

Chen, J, & Lolivret, L. (2011). The determining role of bolus rheology in triggering a swallowing. *Food Hydrocolloids*, *25*(3), 325–332.

Chen, Jianshe. (2009). Food oral processing—A review. *Food Hydrocolloids*, *23*(1), 1–25.

Chen, M., Peele, V. N., Donati, D., Ott, D. J., Donofrio, P. D., & Gelfand, D. W. (1992). Clinical and videofluoroscopic evaluation of swallowing in 41 patients with neurologic disease. *Gastrointestinal Radiology*, *17*(1), 95–98.

Chhabra, R., & Richardson, J. (2011). *Non-Newtonian flow and applied rheology: engineering applications* (2nd ed.). Oxford: Butterworth-Heinemann.

Cichero, J., Jackson, O., Halley, P., & Murdoch, B. (2000). How thick is thick? Multicenter study of the rheological and material property characteristics of mealtime fluids and videofluoroscopy fluids. *Dysphagia*, *15*(4), 188–200.

Claes, J. E., De Maesschalck, L., Huysmans, V., Van Eyck, H., Schittecat, S., Pastuer, M., & Moldenaers, P. (2012). Rheological study of breakfast replacing recipes used in the treatment of dysphagia. *Journal of Texture Studies*, *43*(2), 142–152.

Clavé, P., De Kraa, M., Arreola, V., Girvent, M., Farré, R., Palomera, E., & Serra-Prat, M. (2006). The effect of bolus viscosity on swallowing function in neurogenic dysphagia. *Alimentary Pharmacology & Therapeutics*, *24*(9), 1385–1394.

Coster, S., & Schwarz, W. (1987). Rheology and the swallow-safe bolus. *Dysphagia*, *1*(3), 113–118.

Cox, W. P., & Merz, E. H. (1958). Correlation of dynamic and steady flow viscosities. *Journal of Polymer Science*, *28*(118), 619–622.

Dewar, R. J., & Joyce, M. J. (2006). Time-dependent rheology of starch thickeners and the clinical implications for dysphagia therapy. *Dysphagia*, *21*(4), 264–269.

Doraiswamy, D. (2002). The origins of rheology: a short historical excursion. *Rheology Bulletin*, *71*(1), 1–9.

Ekberg, O., Bülow, M., Ekman, S., Hall, G., Stading, M., & Wendin, K. (2009). Effect of barium sulfate contrast medium on rheology and sensory texture attributes in a model food. *Acta Radiologica*, *50*(2), 131–138.

Ekberg, O., Olsson, R., & Sundgren-Borgstrom, P. (1988). Dysphagia relation of bolus size and pharyngeal swallow. *Dysphagia*, *3*(2), 69–72.

Fauci, A. S., Braunwald, E., & Fuselbacher, K. J. (1998). *Harrison's principles of internal medicine*. *San Francisco, CA* (14th ed.). San Francisco, CA.: McGraw-Hill.

Feigl, K., Tanner, F. X., Edwards, B. J., & Collier, J. R. (2003). A numerical study of the measurement of elongational viscosity of polymeric fluids in a semihyperbolically converging die. *Journal of Non-Newtonian Fluid Mechanics*, *115*(2-3), 191–215.

Ferguson, D., Shuttleworth, A., & Whittaker, D. (1999). *Oral bioscience* (p. 323). Edinburgh: Churchill Livingstone.

Gallegos, C., & Martínez-Boza, F. (2010). Linear viscoelasticity. In *Rheology: Enciclopedia of Life Support Systems (EOLSS), UNESCO*. Oxford.

Garcia, J. M., & Chambers, E. (2010). Managing dysphagia through diet modifications. *The American Journal of Nursing*, *110*(11), 26–33.

Garcia, J. M., Chambers, E., Matta, Z., & Clark, M. (2008). Serving temperature viscosity measurements of nectar- and honey-thick liquids. *Dysphagia*, *23*(1), 65–75.

García-Peris, P., & Parón, L. (2007). Long-term prevalence of oropharyngeal dysphagia in head and neck cancer patients: Impact on quality of life. *Clinical Nutrition*, *26*(6), 710–717.

Germain, I., Dufresne, T., & Ramaswamy, H. S. (2006). Rheological characterization of thickened beverages used in the treatment of dysphagia. *Journal of Food Engineering*, *73*(1), 64–74.

Goulding, R., & Bakheit, A. (2000). Evaluation of the benefits of monitoring fluid thickness in the dietary management of dysphagic stroke patients. *Clinical Rehabilitation*, *14*(2), 119–124.

Groher, M., Crary, M., Carnaby, G., Vickers, Z., & Aguilar, C. (2006). The impact of rheologically controlled materials on the identification of airway compromise on the clinical and videofluoroscopic swallowing examinations. *Dysphagia*, *21*(4), 218–225.

Groher, M. E. (1997). *Dysphagia: Diagnosis and management*. *Dysphagia: Diagnosis and managment. Butterworth-Heinemann Medical* (3rd ed.). Butterworth-Heinemann.

Hamlet, S., Choi, J., Zormeier, M., Shamsa, F., Stachler, R., Muz, J., & Jones, L. (1996). Normal adult swallowing of liquid and viscous material: scintigraphic data on bolus transit and oropharyngeal residues. *Dysphagia*, *11*(1), 41–47.

Hasegawa, A., Otoguro, A., Kumagai, H., & Nakazawa, F. (2005). Velocity of swallowed gel food in the pharynx by ultrasonic method. *Journal-Japanese Society of Food Science and Technology*, *52*(10), 441.

Hiiemae, K. (2004). Mechanisms of food reduction, transport and deglutition: how the texture of the food affects feeding behavior, *35*(315), 171–200.

Ikeda, S., & Nishinari, K. (2001). “Weak Gel”-Type rheological properties of aqueous dispersions of nonaggregated κ-carrageenan helices. *Journal of agricultural and food chemistry*, *49*(9), 4436–4441.

Leder, S. B., Judson, B. L., Sliwinski, E., & Madson, L. (2012). Promoting safe swallowing when puree is swallowed without aspiration but thin liquid is aspirated: nectar is enough. *Dysphagia*, 1–5.

Leder, S. B., & Murray, J. T. (2008). Fiberoptic endoscopic evaluation of swallowing. *Physical medicine and rehabilitation clinics of North America*, *19*(4), 787–801.

Linden, R. (1998). *The scientific basis of eating: taste and smell, salivation, mastication and swallowing, and their dysfunctions* (Vol. 9.). Karger.

Logemann, J. a. (2007). Swallowing disorders. *Best practice & research. Clinical gastroenterology*, *21*(4), 563–73.

Lopes da Silva, J. A., Gonçalves, M. P., & Rao, M. A. (1993). Viscoelastic behaviour of mixtures of locust bean gum and pectin dispersions. *Journal of Food Engineering*, *18*(3), 211–228.

Macosko, C., & Larson, R. (1994). *Rheology: principles, measurements, and applications*. New York, NY: VCH.

Martino, R., Foley, N., Bhogal, S., Diamant, N., Speechley, M., & Teasell, R. (2005). Dysphagia after stroke: incidence, diagnosis, and pulmonary complications. *Stroke; a journal of cerebral circulation*, *36*(12), 2756–2763.

Matta, Z., Chambers, E., Mertz, J. G., & McGowan, J. H. (2006). Sensory characteristics of beverages prepared with commercial thickeners used for dysphagia diets. *Journal of the American Dietetic Association*, *106*(7), 1049–54.

Meng, Y., Rao, M. a., & Datta, A. K. (2005). Computer Simulation of the Pharyngeal Bolus Transport of Newtonian and Non-Newtonian Fluids. *Food and Bioproducts Processing*, *83*(4), 297–305.

Mohnen, D. (2008). Pectin structure and biosynthesis. *Current opinion in plant biology*, *11*(3), 266–277.

Morrison, F. A. (2001). *Understanding Rheology* (Ilustrated., p. 545). Oxford University Press.

Muñoz-Díaz, E. (2012). *Nuevo reómetro de orificio*. (Doctoral dissertation).Universidad Nacional Autónoma de México.

Muñoz-Díaz, E., Solorio-Ordaz, F., & Ascanio, G. (2012). A numerical study of an orifice flowmeter. *Flow Measurement and Instrumentation*, *26*, 85–92.

Naranjo, J. (2010). *Desarrollo y construcción de un reómetro de orificio para determinar propiedades extensionales*. (Doctoral dissertation). Universidad Nacional Autónoma de México.

Nazar, G., Ortega, A., & Fuentealba, I. (2009). Evaluación y manejo integral de la disfagia orofaringea. *Revista médica Clínica Las Condes*, *20*(4), 449–457.

Nguyen, H. N., Silny, J., & Albers, D. (1997). Dynamics of esophageal bolus transport in healthy subjects studied using multiple intraluminal impedancometry. *American Journal of of Physiology-Gastrointestinal and Liver Physiology*, *273*(4), G958–G964.

Nishinari, K. (2000). Rheology of physical gels and gelling processes. *Reports on Progress in Polymer Physics in Japan*, *43*, 163–192.

O'Brien, V., & Mackay, M. (2002). Shear and elongation flow properties of kaolin suspensions. *Journal of Rheology*, *46*, 557.

O'Leary, M., Hanson, B., & Smith, C. (2010). Viscosity and non-Newtonian features of thickened fluids used for dysphagia therapy. *Journal of food science*, *75*(6), E330–E338.

Omari, T. I., Rommel, N., Szczesniak, M. M., Fuentealba, S., Dinning, P. G., Davidson, G. P., & Cook, I. J. (2006). Assessment of intraluminal impedance for the detection of pharyngeal bolus flow during swallowing in healthy adults. *American Journal of of Physiology-Gastrointestinal and Liver Physiology*, *290*(1), G183–G188.

Ozaki, K., Kagaya, H., Yokoyama, M., Saitoh, E., Okada, S., González-Fernández, M., Palmer, J. B., Uematsu, H. (2010). The risk of penetration or aspiration during videofluoroscopic examination of swallowing varies depending on food types. *The Tohoku Journal of Experimental Medicine*, *220*(1), 41–46.

Palaniraj, A., & Jayaraman, V. (2011). Production , recovery and applications of xanthan gum by Xanthomonas campestris. *Journal of Food Engineering*, *106*(1), 1–12.

Payne, C., Methven, L., Fairfield, C., & Bell, A. (2011). Consistently inconsistent: commercially available starch-based dysphagia products. *Dysphagia*, *26*(1), 27–33.

Popa, S., Murith, M., Chisholm, H., & Engmann, J. (2013). Matching the rheological properties of videofluoroscopic contrast agents and thickened liquid prescriptions. *Dysphagia*, *28*(2), 245–52.

Quinchia, L. a., Valencia, C., Partal, P., Franco, J. M., Brito-de la Fuente, E., & Gallegos, C. (2011). Linear and non-linear viscoelasticity of puddings for nutritional management of dysphagia. *Food Hydrocolloids*, *25*(4), 586–593.

Raut, V. V, McKee, G. J., & Johnston, B. T. (2001). Effect of bolus consistency on swallowing--does altering consistency help? *European archives of oto-rhino-laryngology*, *258*(1), 49–53.

Różańska, S., Broniarz-Press, L., Różański, J., Mitkowski, P., Ochowiak, M., & Woziwodzki, S. (2013). Extensional viscosity of o/w emulsion stabilized by polysaccharides measured on the opposed-nozzle device. *Food Hydrocolloids*, *32*(1), 130–142.

Seo, C.-W., & Yoo, B. (2013). Steady and dynamic shear rheological properties of gum-based food thickeners used for diet modification of patients with Dysphagia: effect of concentration. *Dysphagia*, *28*(2), 205–211.

Sopade, P. a., Halley, P. J., Cichero, J. a. Y., & Ward, L. C. (2007). Rheological characterisation of food thickeners marketed in Australia in various media for the management of dysphagia. I: Water and cordial. *Journal of Food Engineering*, *79*(1), 69–82.

Sopade, P. a., Halley, P. J., Cichero, J. a. Y., Ward, L. C., Hui, L. S., & Teo, K. H. (2008). Rheological characterisation of food thickeners marketed in Australia in various media for the management of dysphagia. II. Milk as a dispersing medium. *Journal of Food Engineering*, *84*(4), 553–562.

Stading, M. (2008). Determination of extensional rheological properties by hyperbolic contraction flow (Vol. 1027, pp. 1114–1116).

Stading, M., Edrud, S., & Ekman, S. (2007). Rheological properties of a barium sulphate contrast medium. *Annual Transaction of the Nordic Rheology Society*, *15*, 267–268.

Steele, C. M., Van Lieshout, P. H. H. M., & Goff, D. H. (2003). The Rheology of Liquids: A Comparison of Clinicians? Subjective Impressions and Objective Measurement. *Dysphagia*, *18*(3), 182–195.

Steffe, J. F. (1996). *Rheological methods in food process engineering* (2nd ed.). Michigan: Freeman Press.

Stegemann, S., Gosch, M., & Breitkreutz, J. (2012). Swallowing dysfunction and dysphagia is an unrecognized challenge for oral drug therapy. *International journal of pharmaceutics*, *430*(1-2), 197–206.

Strowd, L., Kyzima, J., Pillsbury, D., Valley, T., & Rubin, B. (2008). Dysphagia dietary guidelines and the rheology of nutritional feeds and barium test feeds. *Chest*, *133*(6), 1397–401.

Stuart, S., & Motz, J. M. (2009). Viscosity in infant dysphagia management: comparison of viscosity of thickened liquids used in assessment and thickened liquids used in treatment. *Dysphagia*, *24*(4), 412–422.

Tan, H., Tam, K. C., Tirtaatmadja, V., Jenkins, R. D., & Bassett, D. R. (2000). Extensional properties of model hydrophobically modified alkali-soluble associative (HASE) polymer solutions. *Journal of Non-Newtonian Fluid Mechanics*, *92*(2-3), 167–185.

Valle, D., Tanguy, P., & Carreau, P. (2000). Characterization of the extensional properties of complex fluids using an orifice flowmeter. *Journal of Non-Newtonian Fluid Mechanics*, *94*(10), 1–13.

Vrentas, C. M., & Graessley, W. W. (1982). Study of Shear Stress Relaxation in Well-Characterized Polymer Liquids. *Journal of Rheology*, *26*(4), 359.

Wendin, K., Ekman, S., Bülow, M., Ekberg, O., Johansson, D., Rothenberg, E., & Stading, M. (2010). Objective and quantitative definitions of modified food textures based on sensory and rheological methodology. *Food & nutrition research*, *54*, 1–11.

Whelan, K. (2001). Inadequate fluid intakes in dysphagic acute stroke. *Clinical nutrition (Edinburgh, Scotland)*, *20*(5), 423–8.

Willats, W. G., Knox, J. P., & Mikkelsen, J. D. (2006). Pectin : new insights into an old polymer are starting to gel. *Trends in Food Science & Technology*, *17*(3), 97–104.